University ID : 10532   Students ID : LB2012039

Subject Index : TN929   Security Level : Normal

HUNAN UNIVERSITY

PhD THESIS

EXPERIMENT INVESTIGATION OF PAPR REDUCTION SCHEMES IN THE INTENSITY MODULATION DIRECT DETECTION OPTICAL OFDM SYSTEM

Student name   :   MAI VAN LAP

College   : Computer Science and Electronic Engineering

Supervisor   :   Professor CHEN LIN

Major   :   Computer Science and Technology

Research field :   Optical Communication

Date   :   September, 2015

湖南大学博士学位论文

强度调制直接检测光 OFDM 系统中 PAPR

抑制方案的实验研究

学位申请人姓名 ：	MAI VAN LAP
培养单位　　　：	信息科学与工程学院
导师姓名及职称：	陈 林 教授
专业名称　　　：	计算机科学与技术
研究方向　　　：	光纤通信
论文提交日期　：	2015 年 9 月 25 日
论文答辩日期　：	2015 年 12 月 14 日
答辩委员会主席：	

Research on Experiment Investigation
of PAPR reduction schemes in the Intensity Modulation
Direct Detection Optical OFDM system

By

MAI VAN LAP

M.S. (Hanoi National University, Vietnam) 2006

A dissertation submitted in partial satisfaction of the

Requirements for the Degree of

Doctor of Philosophy of Engineering

in

Computer Applications Technology

in the

Graduate school

Of

Hunan University

Supervisor

Professor CHEN Lin

September, 2015

HUNAN UNIVERSITY DECLARATION

I, MAI VAN LAP hereby declare that the work presented in this PhD thesis entitled "Experiment investigation of PAPR reduction schemes in the Intensity Modulation/Direct Detection Optical OFDM system" is my original work and has not been presented elsewhere for any academic qualification. Where references have been used from books, published papers, reports and web sites, it is fully acknowledged in accordance with the standard referencing practices of the discipline.

Student's signature:＿＿＿＿＿　　　Date:＿＿＿＿＿

Copyright Statement

Permission is herewith granted to Hunan University to circulate and reproduce for non-commercial purposes, at its discretion, this thesis upon the request of individuals or institutions. The author does not reserve other publication rights and the thesis nor extensive extracts from it be printed or otherwise reproduce without the author's written permission.

This thesis belongs to:

    1. Secure   ☐, and this power of attorney is valid after

    2. Not secure ☐.

    （Please mark the above corresponding check box with "√"）

Author's Signature : ＿＿＿＿＿   Date: ＿＿＿＿＿

Supervisor's Signature : ＿＿＿＿＿   Date: ＿＿＿＿＿

DEDICATION

This thesis is dedicated to my great family.

ABSTRACT

In recent years, optical orthogonal frequency division multiplexing (OOFDM) has emerged as a dominant research and development area in the field of high-speed optical communications. OFDM is a potential candidate as the most promising next-generation optical networks such as passive optical networks and optical transport networks, due to their simple configuration based on low cost, high speed data rates, high spectral efficiency, high quality of service and robustness against narrow band interference, frequency selective fading, and chromatic dispersion. However, intensity modulation - direct detection (IM/DD) OOFDM is known to be susceptible to high peak-to-average power ratio (PAPR) and chromatic dispersion (CD). When the optical launch power is relative high, high PAPR will cause distortion in both electrical and optical devices, resulting in the fiber nonlinear effects.

In this thesis, we propose three IM/DD optical OFDM systems and develop some algorithms to reduce the fiber nonlinearity through reducing the high PAPR of the optical OFDM signal. Our innovation works are as follows:

Firstly, a new spreading code is proposed to reduce the PAPR in intensity modulation direct detection optical OFDM system. The new spreading code with low cross-correlation and high auto-correlation can be capable of supporting $2N+1$ users. It means that $2N+1$ users or data symbols are able to be transmitted over only N sub-carriers. The new spreading code can be used to reduce PAPR and expand the capable of channel in spread OFDM systems. The experimental results showed that, after transmission over 70 km single-mode fiber (SMF), at the bit error rate (BER) of 1×10^{-3} for 1.726 Gb/s BPSK new spreading signal and 1.718 Gb/s 4QAM original signal, the receiver sensitivity of new spreading signal can be improved by 2.1 dB, with fiber launch power of 2.75 dBm. Meanwhile the PAPR can be reduced by about 4.6 dB, when compared with the original OFDM signal at a CCDF of 10^{-4}. The results also prove that new spreading code has low cross correlation and has better orthogonality property proportional to the high number of subcarrier.

Secondly, a new hybrid method based on Carrier Interferometry (CI) codes and companding transform is proposed in the IM/DD optical OFDM system. The CI codes can spread each of the N low-rate symbol streams across all N subcarriers and orthogonal CI spreading codes are used before the IFFT stage. Thus, it has frequency

diversity benefits for each symbol stream, which can lead to good BER performance. Additionally, the use of orthogonal CI spreading codes can eliminates high peaks of power distribution, resulting in alleviating PAPR concerns. To get more efficient performances of system, the companding technique is adopted after the IFFT stage. The companding technique can reduce PAPR and improve BER performance with the simple implementation and low computational complexity. Subsequently, we experimentally demonstrated the new hybrid method in an IM/DD OOFDM system, and the experiment results show that the proposed method can not only reduce PAPR but also obtain the better BER performance. The PAPR of hybrid signal has been reduced by about 5.7 dB when compared to the original system at a CCDF of 10^{-4}. At a bit error rate (BER) of 10^{-4} for 1.718 Gb/s 4QAM OFDM signals, after transmission over 100 km single mode fiber (SMF), the receiver sensitivity is improved by 3.7, 4.2, and 5 dB with launch powers of 3, 6, and 9 dBm, respectively.

Finally, a novel binary particle swarm optimization (NBPSO) method based on dummy sequence insertion (DSI) is proposed and experimentally demonstrated for PAPR reduction in the IM-DD OOFDM system. The dummy sequence is inserted for only PAPR reduction. The most important feature of DSI method is finding the qualified dummy sequence. The new binary particle swarm optimization (NBPSO) method can generate high-quality solution within shorter calculation time on getting more qualified dummy sequence. The experiment results show the effectiveness of the proposed scheme. The PAPR of proposed scheme has been reduced by about 2.8 dB when compared to the regular system at a CCDF of 10^{-4}. At a BER of FEC 3.8×10^{-3} for 6.23Gb/s 16QAM OFDM signals, after transmission over 100 km single mode fiber (SMF), the receiver sensitivity is improved by 1.9 and 3.2 dB with launch powers of 2 and 8 dBm, respectively.

详细中文摘要

近年来，在高速光通信系统中，光正交频分复用（OOFDM）技术已成为人们主要的研究方向和发展趋势。OFDM 技术是无源光网络及光传输网等下一代光网络中最有潜力的技术之一，这是由于 OFDM 技术具有成本低、高传输速率、高频谱效率、高服务质量等优势，同时具有很强的鲁棒性来抵抗窄带串扰、频率选择性衰落和色散。然而，众所周知，强度调制/直接检测 OOFDM 系统对高峰均功率比和色散十分敏感。当光发射功率相对高，高 PAPR 使信号在电子及光学器件中产生失真，同时导致光纤中的非线性效应。

在本论文中，我们提出了三种 IM/DD 光 OFDM 系统，同时提出一些算法通过降低光 OFDM 信号的高 PAPR 来减少光纤的非线性效应。创新性工作如下：

首先，在强度调制直接检测光 OFDM 系统中提出了一种新的扩频码，以降低 PAPR。新扩频码具有低互相关和高自相关性，能够支持 $2N+1$ 个用户。也就是说可以只通过 N 个子载波发送 $2N+1$ 个用户或数据符号。新扩频码可用于降低 PAPR，扩展扩频 OFDM 系统的信道容量。实验结果表明，在单模光纤中传输 70 km 后，当误码率为 1×10^{-3} 时，1.726 Gb/s 的 BPSK 新扩频信号的接收灵敏度比 1.718 Gb/s 的 4QAM 信号的接收灵敏度提升了 2.1 dB，光纤发射功率为 2.75 dBm。同时当 CCDF 为 10^{-4} 时，与原始 OFDM 信号相比较，PAPR 可降低约 4.6 dB。研究结果还证明新的扩频码具有较低的互相关性，以及当子载波数量较大时，具有良好的正交性。

其次，在 IM/DD 光 OFDM 系统中，提出了基于载波干涉（CI）码和压扩变换的新的混合方法。载波干涉码可以使每段 N 个低速比特流在所有 N 个子载波中延展，且正交的 CI 扩频码是在进行 IFFT 之前使用。因此对每个符号数据流可以进行频率分集，使得具有更好的误码性能。另外，使用正交 CI 扩频码可以消除高功率峰值，缓解 PAPR 的问题。在 IFFT 后采用压扩技术可以使系统获得更高的效率和性能。该压扩技术可以降低 PAPR，同时实现简单，具有较低的计算复杂度，改善误码性能。随后，我们用实验在 IM/DD OOFDM 系统中验证了新的混合方法，实验结果表明，该方法不仅可以降低 PAPR，而且获得了较好的误码性能。当 CCDF 为 10^{-4} 时，与原始系统相比，采用混合方法的信号 PAPR 降低

了约 5.7 dB。当误码率为 10^{-4} 时，1.718 Gb/s 的 4QAM OFDM 信号在单模光纤中传输 100 km 后，对应发射功率分别为 3、6 和 9dBm 时，接收机灵敏度分别提升了 3.7、4.2 和 5 dB。

最后，在 IM/DD OOFDM 系统中，提出了一种基于虚拟序列插入（DSI）的新型二元粒子群算法（NBPSO）方法，并采用实验验证了该方法对降低 PAPR 的可行性。虚拟序列的插入仅用于降低 PAPR。DSI 方法的最重要的特征是找到符合条件的虚拟序列。新的二进制粒子群算法（NBPSO）可以在更短的时间内获得更符合条件的虚拟序列的高质量的解决方案。实验结果表明该方案具有有效性。与常规系统相比，当 CCDF 为 10^{-4} 时，提出方案的 PAPR 可以降低约 2.8 dB。在单模光纤中传输 100 km 后，FEC 误码率门限值达到 3.8×10^{-3} 6.23 Gb/s 的 16QAM OFDM 信号，当发射功率分别为 2 和 8 dBm 时，接收机灵敏度分别提高了 1.9 和 3.2 dB。

关键词：强度调制/直接检测，光正交频分复用，载波干涉码，新的扩频码，PAPR，新型二元粒子群，虚拟序列插入，单模光纤

。

TABLE OF CONTENTS

LIST OF FIGURES

LIST OF TABLES

Chapter 1: **INTRODUCTION**

1.1 Optical OFDM

Orthogonal frequency division multiplexing (OFDM), an efficient multi-carrier modulation scheme with numerous advantages, has been employing in a wide variety of wired and wireless communication standards including wireless LAN networks (HIPERLAN/2, IEEE 802.11a, IEEE 802.11g); Worldwide Interoperability for Microwave Access (WiMax - IEEE 802.16); Digital Subscriber Line (DSL) and Digital Audio and Video Broadcast (DAB, DVB).

OFDM, having been established as the physical interface of choice for these communication standards, has only recently made a transition to the optical communications community [1, 2]. A major hindrance to this transition has been the differences between conventional OFDM systems and conventional optical systems. In conventional OFDM systems, the signal is bipolar and the information is carried on the electrical field while in a typical optical system, the signal is unipolar and the information is carried on the intensity of the optical signal.

However, advancements in silicon technology supported by Moore's law, together with increased demand for higher data rates across long fiber distances have facilitated the emergence of OFDM in optical communications [3].

For optical communications, OFDM has demonstrated resilience to transmission impairments arising from fiber polarization mode dispersion and chromatic dispersion. It has been shown that provided the delay spread caused by chromatic dispersion is less than the cyclic prefix interval, OFDM can easily compensate for dispersion-induced impairments [4]. This is no trivial advantage when one considers the fact that as data rates increase, chromatic dispersion increases with the square of the data rate while polarization mode dispersion (PMD) increases linearly with the data rate [5].

Consequently, at such high data rates, the computational requirements involved in electronic dispersion compensation for serial modulation formats may become impractical, particularly in access networks [6]. Another important advantage of OFDM worthy of note is the increase in spectral efficiency that can be obtained from using higher modulation formats [7].

By being able to apply the afore-mentioned advantages of OFDM into the optical domain, OFDM has demonstrated research potential for a wide variety of applications in the core, metro and access networks.

The research about Optical OFDM is mainly classified into two main categories: coherent detection [8] and direct detection [9, 10] according to their underlying techniques and applications.

In coherent detection systems, the detection of the optical OFDM signal is carried out using coherent mixing between the incoming signal and a local oscillator. Coherent optical OFDM has great sensitivity and spectral efficiency and also susceptible to polarization mode dispersion (PMD). Unfortunately, these great benefits of CO-OFDM are accompanied by high-cost installations, including narrow line-width laser sources, local oscillators, 90^0 optical hybrids, and extra signal processing accounting for the phase and frequency offset estimations [11, 12].

In IM/DD optical OFDM systems, the signal is usually transmitted with intensity modulation, and then received with square law detection. The DDO- OFDM can be accommodated with a low-cost DFB laser of megahertz-level line-width [6], eliminates the local oscillators and optical hybrids, and need not estimate the phase and frequency offsets, therefore making the DDO-OFDM quite convenient to be implemented. Consequently, compromising the installation complexity and the transmission performance, the DDO-OFDM would be an alternative format for optical transmission. The IM/DD optical OFDM is one of the most promising candidates for the next-generation optical networks such as passive optical networks [13] and optical transport networks [14].

Comparing with coherent optical OFDM, the IM/DD Optical OFDM is advantageous in terms of complexity and easy configuration. Simple direct detection significantly reduces the system complexity and tolerates the fiber dispersion. IM/DD optical OFDM is one of the promising candidates for cost-sensitive optical access networks. However, IM/DD optical OFDM is known to be susceptible to high peak-to-power ratio (PAPR) and chromatic dispersion (CD). High PAPR will cause distortion in electrical and optical devices and introduce fiber nonlinear effects when the power traveling through the fiber transmission is very high in IM/DD Optical OFDM. Thus, it is necessary to focus on the IM/DD optical OFDM transmission limits in presence of high PAPR and chromatic dispersion. Furthermore, it is in public interest to develop

algorithms and techniques and propose new experimental setups to reduce the high PAPR, to decrease the fiber nonlinearity effects. Therefore, this thesis focuses on topics in relation to high spectral efficiency IM/DD optical OFDM over SMF link.

1.2 Thesis organization

A common structure is used throughout this thesis. Each chapter begins with an introduction where the aims and contents of the chapter are highlighted, and is concluded with a summary of the main contributions of the chapter.

The organization of this thesis is given as follows:

Chapter 2

This chapter intends to give an introduction on OFDM modulation, from its fundamentals mathematical modeling to the transmitter and receiver compositions. A briefly review of the concept Optical OFDM is presented. The key optical components used in optical OFDM systems are discussed and the two major variants of optical OFDM such as coherent optical OFDM and IM/DD optical OFDM are been described.

Chapter 3

In this chapter a novel technique based on new spreading code is proposed to reduce the high PAPR in IM/DD optical OFDM. Using the proposed system, the fiber nonlinearity can be decreased when comparing with original system. An experimental setup is proposed to verify the theoretical investigations.

Chapter 4

In order to improve the received sensitivity of the system, in this chapter we propose a new hybrid based on carrier interferometry codes and companding technique to reduce PAPR and impair the nonlinearity of components in optical OFDM system. The experimental results show the nonlinearity of components improvement when fiber launch power increases.

Chapter 5

As well as chapters 3, and 4 focus on PAPR reduction in the IM/DD OOFDM system, in this chapter we propose a novel can reduce the PAPR while decreasing the complexity of system. This novel is new binary particle swarm optimization (NBPSO) on dummy sequence insertion (DSI) method for PAPR reduction in an IM/DD optical

OFDM system without any side information. Experimental demonstration show better performance.

Chapter 6

This chapter summarizes the thesis and gives new directions for future work.

1.3 Contribution of the thesis

The contributions of this thesis are presented in chapter 3-6 and listed as follows:

Chapter 3:

A novel technique for PAPR reduction in IM/DD optical OFDM system based on new spreading code is proposed. The new spreading code with low cross-correlation and high auto-correlation while capable of supporting $2N+1$ users or data symbols is investigated. The proposed technique is experimentally demonstrated over 70 km single-mode fiber (SMF) transmission with number of subcarrier is 256 and 512. The results shown that, the proposed technique can reduce the PAPR and improve the received sensitivity compared with original system. The result also prove that new spreading code has better orthogonality property proportional to the high number of subcarrier. With the same subcarrier, at the bit error rate (BER) of 1×10^{-3} for 1.726 Gb/s BPSK proposed signal and 1.718 Gb/s 4QAM original signal, the receiver sensitivity of proposed signal can improve by 2.1 dB, when fiber launch power of 2.75 dBm. The PAPR can reduce by about 4.6 dB, when compared with the original OFDM signal at a complementary cumulative distribution function (CCDF) of 10^{-4}.

Chapter 4:

A new hybrid method is proposed for PAPR reduction in IM/DD optical OFDM system. This hybrid based on Carrier Interferometry (CI) codes combined with companding transform. The brief structure of CI codes and companding transform are presented, and an end to end signal processing is mathematically investigated. The effect of our proposed hybrid in the BER performance of the system has been experimentally demonstrated over 100 km SMF with different launch powers. At a CCDF of 10^{-4}, the PAPR of OFDM signal with the hybrid method is reduced by 5.7 dB, while with the CI codes and the companding technique are reduced by 3.1 and by 2.8 dB, respectively comparing with the original OFDM. The experimental results show that, at the same fiber launch power, the receiver sensitivity of optical OFDM signal

with the hybrid method is better than signal with CI codes, with companding technique and with the original OFDM. At the BER of 10^{-4} for 1.718 Gb/s 4QAM OFDM signal, the received power of optical OFDM signal with hybrid method is more sensitive than the original OFDM by 3.7, 4.2, and 5 dB in case of 3, 6, 9 dBm fiber launch power, respectively. It can be clearly seen that the proposed system can improve the received sensitivity when the optical launch power is increasing.

Chapter 5:

A novel binary particle swarm optimization (NBPSO) method based on dummy sequence insertion (DSI) is proposed and experimentally demonstrated for PAPR reduction in the IM-DD OOFDM system. The specified dummy sequence is inserted only for PAPR reduction and without any side information. The key to enhance its performance is creating more qualified dummy sequence. The novel binary particle swarm optimization method can find more qualified dummy sequence. In this way, it can be used to mitigate the PAPR problem in OFDM system effectively. The experiment results show that, at the BER of FEC 3.8×10^{-3} for 6.23 Gb/s 16QAM signals after transmission over 100 km SMF, the received power with proposed technique is more sensitive than the original by 1.9 and 3.2 dB in case of 2, and 8 dBm fiber launch powers, respectively. At the CCDF of 10^{-4}, the PAPR reduced by more 2.8 dB compared to conventional system.

Chapter 2: **OPTICAL OFDM SYSTEM**

2.1 Introduction

As stated in Chapter 1, an increase in demand for high data rates has been an important factor in the emergence of OFDM in the optical domain, with a wide variety of solutions developed for the next generation network. This emergence has been facilitated by the intrinsic advantages of OFDM such as its high spectral efficiency, ease of channel and phase estimation; and robustness against delay [15].

This chapter gives an overview of optical OFDM system from the basic concept of OFDM to its robust applications. A history and applications of OFDM will be discussed, and then the fundamentals of OFDM including its basic units will be presented. After a brief discussion about the advantages and disadvantages of OFDM, the basic concept of the integration of OFDM in optical communications will be presented including the optical transmission link, the optical and electrical devices used according to the detection process such as coherent detection or direct detection. Finally a comparison between coherent optical OFDM and IM/DD optical OFDM will be shown.

2.2 OFDM review

2.2.1 History of OFDM and its applications

Figure 2.1 shows the historical development for both theoretical basis and practical application of OFDM across a range of communication systems [16]. The first proposal to use orthogonal frequencies for transmission appears in a 1966 patent by Chang of Bell Labs [17]. The proposal to generate the orthogonal signals using an FFT came in 1969 [18]. The cyclic prefix (CP),which is an important aspect of almost all practical OFDM implementations, was proposed in 1980 [19]. These are the three key aspects that form the basis of most OFDM systems. The breakthrough papers by Telatar and Foschini on multiple antenna systems fuelled another wave of research in OFDM [20, 21]. Although the capacity gains of these multiple-input–multiple-output (MIMO) systems do not theoretically depend on any particular modulation scheme, the ability to combat dispersion and the good scalability of OFDM become even more important in this context. OFDM began to be considered for practical wireless applications in the mid–

1980s. Cimini of Bell Labs published a paper on OFDM for mobile communications in 1985 [22], while in1987, Lassalle and Alard [23] based in France considered the use of OFDM for radio broadcasting and noted the importance of combining forward error correction (FEC) with OFDM. Because of this interrelationship, OFDM is often called Coded OFDM (C-OFDM) by broadcast engineers. The application of OFDM for wire line communications was pioneered by Cioffi and others at Stanford who demonstrated its potential as a modulation technique for digital subscriber loop (DSL) applications [24]. OFDM is now the basis of many practical telecommunications standards including wireless local area networks (LAN), fixed wireless [25] and television and radiobroadcasting in much of the world [26]. OFDM is also the basis of most DSL standards, though in DSL applications the baseband signal is not modulated onto a carrier frequency and in this context OFDM is usually called discrete multi-tone (DMT). The application of OFDM to optical communications has only occurred very recently, but there are an increasing number of papers on the theoretical and practical performance of OFDM in many optical systems including radio over fiber wireless [27], signal mode optical fiber [28], multimode optical fiber [29], plastic optical fiber [30], and real time optical systems [31].
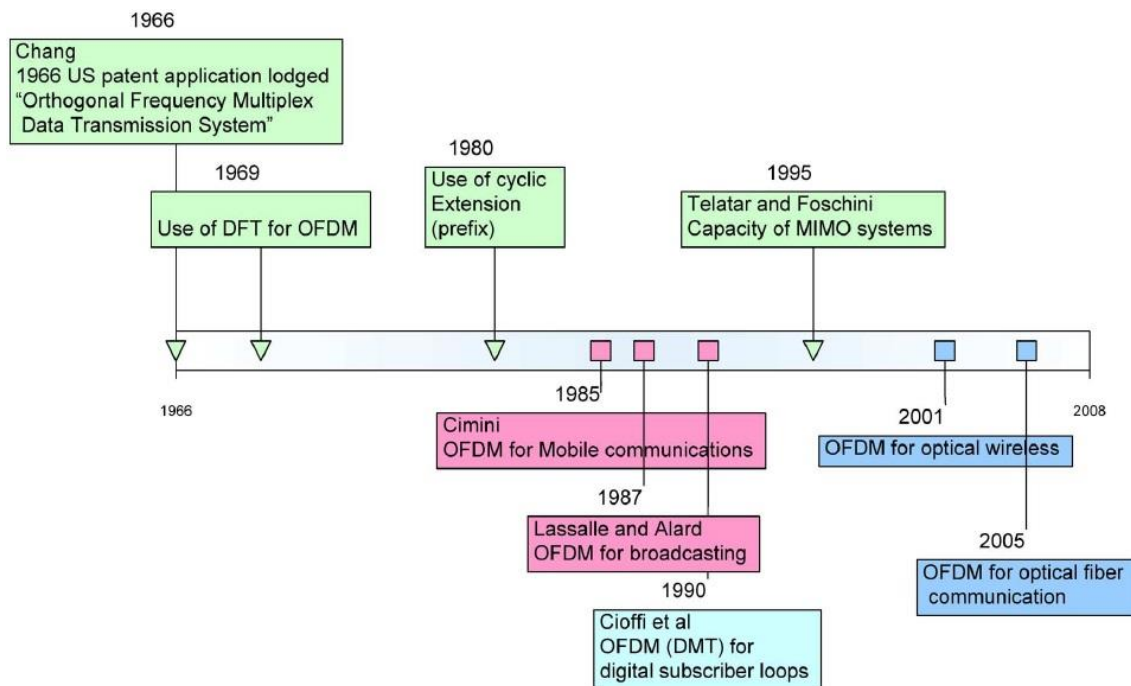
Figure 2.1 History of OFDM

2.2.2 OFDM principles

The OFDM system is a multi-carrier modulation system such as frequency division multiplexing (FDM) systems; the modulated carrier occupies only a fraction of the total bandwidth. In such systems, the transmitted information at a high data rate is divided into N lower-rate parallel streams, each of these streams simultaneously modulating a different subcarrier. If the total data rate is R_s, each parallel stream would have a data rate equal to R_s/N. This implies that the symbol duration of each parallel stream is N x T_s times longer than that the serial symbol duration; and much greater than the channel delay spread τ. These systems are thus tolerant to ISI and are increasingly being employed in modern communication systems where high data rates are used and saving of limited spectrum is of utmost importance.

The OFDM system is the orthogonality of the subcarriers. A set of subcarriers, given by $s_n(t) = e^{j(2\pi f n t)}$ where $n = -N/2 + 1,…, N/2$ and $0 \leq t \leq T$ are said to be orthogonal in the time domain if the following equation holds:

$$\langle S_k(t), S_l(t) \rangle = \int_0^T S_k(t), S_l^{*}(t)dt = \int_0^T e^{j2\Pi(k-l)\Delta ft}dt = T\delta_{k,l} \qquad (2.1)$$

Where $\delta_{k,l}$ is the Kronecker delta defined by:

$$\delta_{k,l} = \begin{cases} 1, & if \ k = l \\ 0, & if \ k \neq l \end{cases} \qquad (2.2)$$

In order for the orthogonality to exist between the subcarriers, the following conditions are necessary:

➤ The frequency of each subcarrier must be chosen such that each subcarrier has an integer number of cycles within the OFDM symbol duration.

➤ The difference in the number of cycles per OFDM symbol for adjacent subcarriers must be one.

For these two conditions to be met, the frequency separation between adjacent subcarriers has to be the inverse of the OFDM symbol duration T.

Figure 2.2 shows the conceptual diagram of multicarrier modulation transmission system. Data symbol is transmitted into N parallel channels with different frequencies. At the receiver, an analogue low-pass filter is used to recover the individual subcarriers.
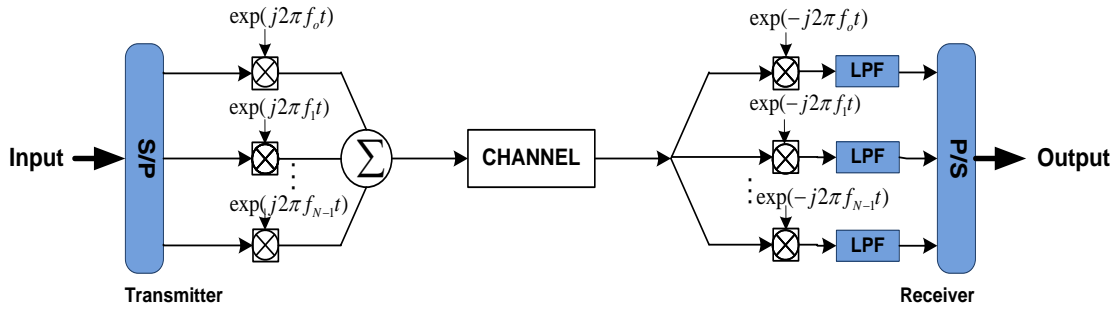
Figure 2.2 Diagram conceptual of Multicarrier transmission, S/P: serial-to-parallel, P/S: Parallel-to-serial, LPF: Low-Pass Filter.

In FDM systems, in order to prevent one subcarrier's spectrum from interfering with another, and to ensure accurate individual demodulation of subcarriers using filters, its require guard bands between the modulated subcarriers. The use of these guard bands results in poor spectral efficiency [32]. OFDM is a special case of FDM which makes use of orthogonal subcarriers. The FDM signal and OFDM signal in the frequency domain are shown in Figure 2.3.

In OFDM, the spectra of the subcarriers are overlap, resulting in saving of bandwidth.
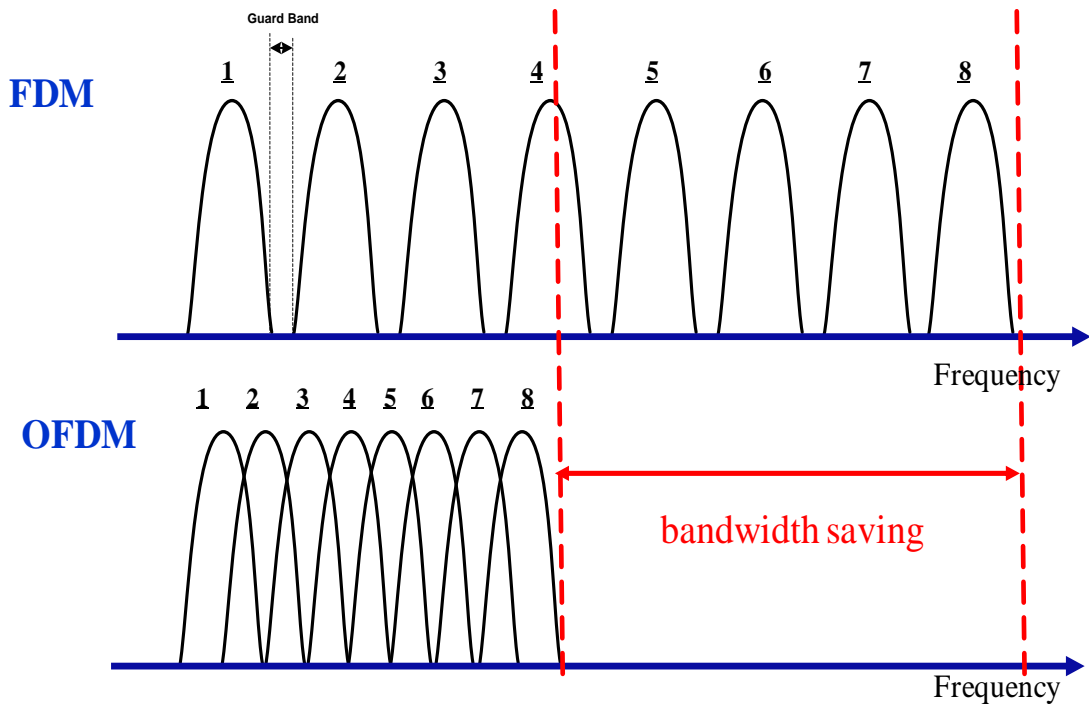
Figure 2.3: OFDM Spectrum versus FDM spectrum

1. Mathematical representation of an OFDM signal

The complex envelope of an OFDM signal, ignoring the cyclic prefix, can be represented mathematically as:

$$S(t) = \sum_{k=-\infty}^{+\infty} \sum_{n=\frac{-Nsc}{2}+1}^{\frac{Nsc}{2}} a_{n,k} g_n(t-kT) \tag{2.3}$$

$$g_n(t) = \frac{1}{\sqrt{T}} e^{j\frac{2\pi nt}{T}} , \ t \in [0,\text{T}] \tag{2.4}$$

where $a_{n,k}$ is the complex symbol transmitted on n^{th} the OFDM subcarrier at the kth signaling interval, $g_n(t\text{-}kT)$ is the complex subcarrier, T is the OFDM symbol period, and N_{sc} is the total number of OFDM subcarriers.

For each OFDM symbol, the nth recovered complex symbol, $\hat{a}_{n,k}$ at the kth signaling interval is given by:

$$\hat{a}_{n,k} = \frac{1}{\sqrt{T}} \int_0^T r(t).g_n^*(t-kT)dt \tag{2.5}$$

where $r(t)$ is the received OFDM signal, the superscript "*" carries out the complex conjugation operation, and all other terms are as defined in section 2.2.3. Equation (2.5) shows that each complex symbol is recovered by multiplying the OFDM symbol by the complex conjugate of the particular subcarrier and integrating over the signaling interval.

2. OFDM system implementations

An OFDM system can be implemented both in continuous time and discrete time. The continuous-time implementation of OFDM makes use of a bank of oscillators, one oscillator for each subcarrier. At the transmitter, the incoming information stream is mapped into symbols depending on the modulation format used (n-PSK or n-QAM) and then fed into a serial-to-parallel conversion block. Each parallel stream at the output of the serial-to-parallel conversion block is used to modulate the corresponding subcarrier simply by multiplication with that particular subcarrier. As stated in section 2.2.2, the frequencies of adjacent subcarriers must differ by $1/T$ to maintain orthogonality. At the receiver, the received signal is correlated by the same subcarriers to give the original transmitted symbols. The OFDM symbol with four subcarriers in Frequency domain and Time domain are shown in Figure 2.4

As we can see in Figure 2.4, the spectra of the subcarriers are *sinc*-shaped and overlap, where the *sinc* function is defined as:

$$\sin c(x) = \frac{\sin(\pi x)}{\pi x} \tag{2.6}$$
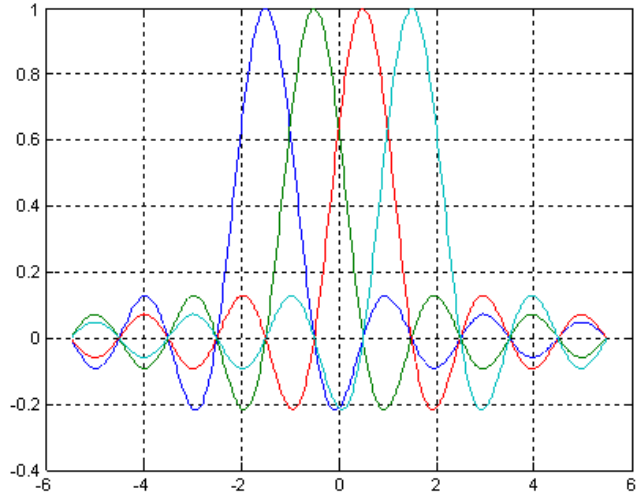
(a)
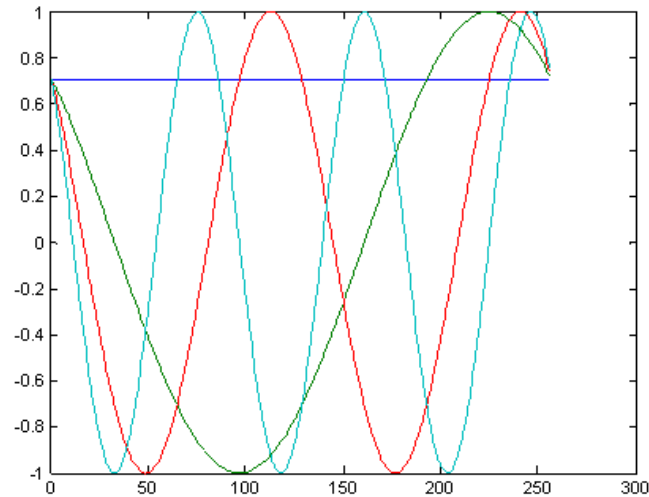
(b)

Figure 2.4: OFDM symbol with four subcarriers: (a): Frequency domain, (b): Time domain

As seen in figure 2.4 (a), we can note that each OFDM subcarrier has significant side lobes over o frequency range which includes many other subcarriers. In OFDM system, the signal is mathematically orthogonal over one OFDM symbol period. The orthogonality between subcarriers can be also explained as the peak of each subcarrier spectrum being of the position of a zero value of the other subcarrier spectrum.

Therefore, compared with others multicarrier Modulation scheme, OFDM is better in low complexity and high spectral efficiency.

On the other hand, the discrete-time OFDM implementation extends the ideas introduced by the continuous-time model into the digital domain by making use of the Discrete Fourier Transform (DFT) and the Inverse Discrete Fourier Transform (IDFT). The concept of using the IDFT and DFT to carry out OFDM modulation and demodulation was first proposed by Weinsten and Ebert in 1971 [33].

The DFT is defined on the N-long complex sequence $x=(x_j, \ 0{\le}j{\le}N$) as[34]:

$$F_k(x) = \frac{1}{\sqrt{N}} \sum_{n=0}^{N-1} x_n \exp\left(\frac{-j2\pi kn}{N}\right), \text{ for } 0 \le k \le N-1 \qquad (2.7)$$

The IDFT is defined as:

$$F_k^{-1}(x) = \frac{1}{\sqrt{N}} \sum_{n=0}^{N-1} x_n \exp\left(\frac{j2\pi kn}{N}\right), \text{ for } 0 \le k \le N\text{-}1 \qquad (2.8)$$

Thus, it can be said that the discrete value of the transmitted OFDM signal, $F(x)$ is merely a simple N-point IDFT of the information symbol, x_n . In reality, due to the large number of complex multiplications involved in computing the DFT and the IDFT, OFDM modulation and demodulation are accomplished more efficiently with the Inverse Fast Fourier Transform (IFFT) and the FFT. By using the IFFT and FFT, the number of complex multiplications is reduced from N^2 to $(N/2).\log_2(N)$ using radix-2 algorithm and form N^2 to $(3/8).N.\log_2(N\text{-}2)$ using a radix-4 algorithm [32].

Compared to the oscillator-based OFDM implementation, the discrete-time implementation is less complex because a large number of orthogonal subcarriers can be easily modulated and demodulated by using the IFFT and FFT without having to resort to having a huge bank of oscillators. The discrete-time OFDM architecture is shown in Figure 2.5. Figure 2.5 shows a block diagram of an OFDM system including an OFDM transmitter, and OFDM receiver and a Channel.

As shown in figure 2.5, at the transmitter, a high digital data stream is split into N parallel streams using a serial-to-parallel converter. Then, each data stream is mapped into a symbol stream using some modulation schemes such as QPSK, n-QAM, n-PSK. IFFT is used to modulate the symbols onto subcarriers and transform the symbol from frequency domain to time domain. The data streams are converted back to one high data stream using parallel-to-serial converted. Cyclic prefix is added to the OFDM

symbol to overcome the inter symbol interference (ISI). A digital-to-Analogue converter is used to put the signal in an analogue form. The baseband signal from the output of the DAC is then up-converted in frequency and transmitted into the channel.
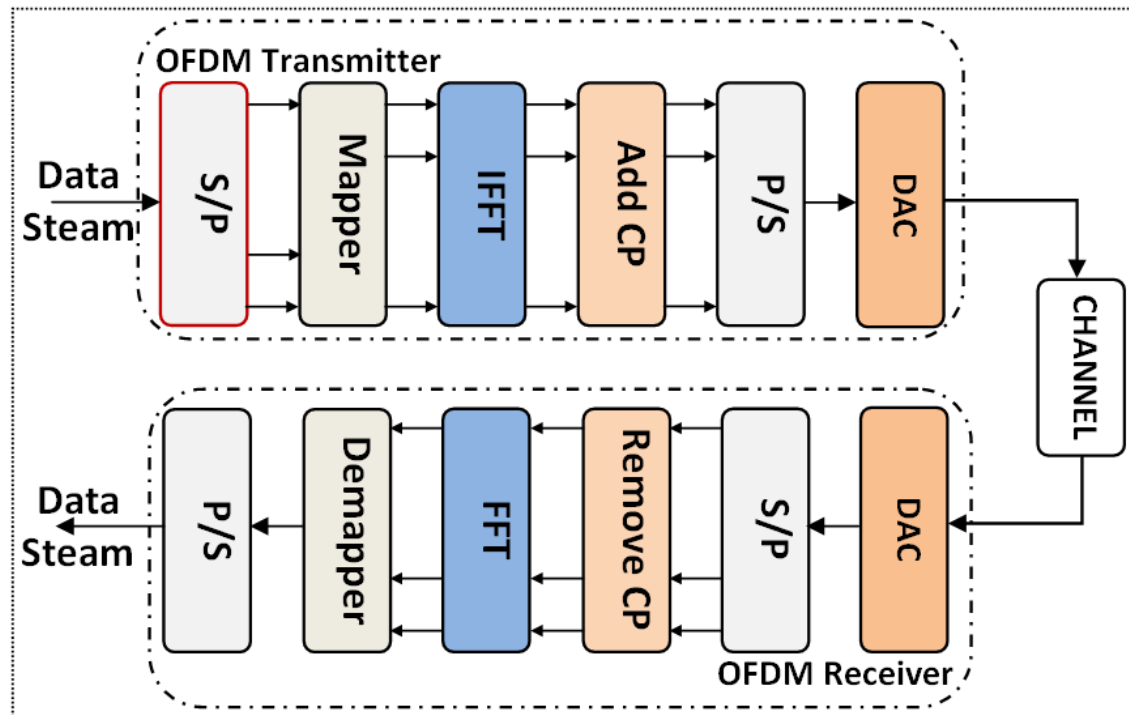
Figure 2.5: Block diagram of an OFDM transceiver. IFFT: Inverse Fast Fourier Transform. DAC: Digital-to-analogue converter. ADC: Analogue-to-digital converter. FFT: Fast Fourier Transform

At the receiver, signal is down-converted to baseband signal and then converted from analogue to digital using and analogue to digital converter (ADC). After removing the CP, a serial-to-parallel converter is used to divide the high data stream to N low data steam. Then the samples pass through a FFT block. After the conversion into frequency domain by FFT, an equalization process is used before de-mapping. Finally data are detected and converted to a high data stream.

1.1 Serial-to-parallel and parallel-to-Serial conversion

In OFDM system, to makes optimal use of the frequency spectrum, each channel can be divided into various subcarriers. Serial-to-parallel converter is used to convert the high data stream into several parallel low data streams. On the other hand, the parallel-to-serial converter is used to convert back the low data streams into one high data stream. Once the low data stream has been divided among the individual subcarriers, each subcarrier is modulated.

1.2 Modulation/Demodulation techniques

The modulation technique can be defined as a mapping of data to a real and imaginary constellations, also called In phase and Quadrature (I/Q) constellations. Figure 2.6 shows some examples of digital modulation technique. For example for a subcarrier modulation of BPSK each subcarriers carries 1 bits of data, QPSK have 2 bits of data, 8-QAM carries 3 bits of data, 16-QAM has 4 bits of data. Each data is mapped into one unique location in the constellation. In the demodulation process, the received IQ symbol is DE mapped back to data word.
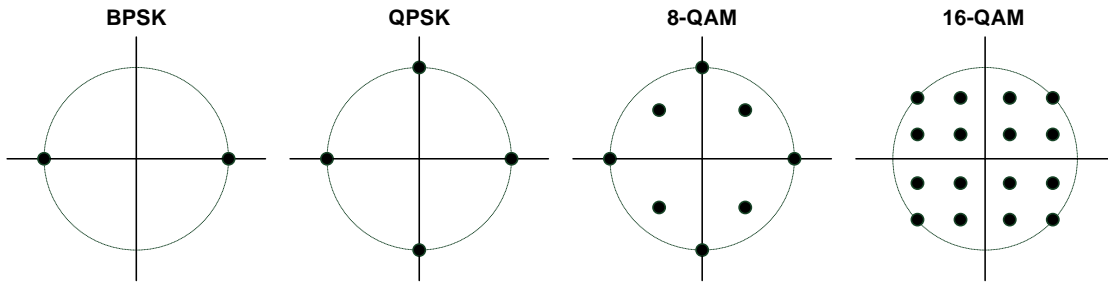
Figure 2.6: Example of digital modulation techniques

1.3 IFFT/FFT implementation in OFDM

IFFT Block at the transmitter and FFT block at the receiver are the main components of the OFDM system. At the transmitter, IFFT is used to modulate data from frequency domain to time domain.

FFT is used in the receiver to recover the original data i.e. to convert back the signal into frequency domain. IFFT and FFT are the blocks which can distinguish the OFDM system from single carrier system.

The input of an IFFT block is a complex vector given by:

$$X = [X_0, X_1, X_2, ..., X_{N-1}]^T \tag{2.9}$$

where N is the IFFT size and X_k is the data to be carrier in the kth OFDM subcarrier. The output of the IFFT is complex vector $x=[x_0, x_1, x_2, ..., x_{N-1}]^T$ which can be obtained using the inverse discrete Fourier transform given by:

$$x_n = \frac{1}{\sqrt{N}} \sum_{k=0}^{N-1} X_k \exp\left(\frac{j2\pi kn}{N}\right), \text{ for } 0 \leq n \leq N\text{-}1 \tag{2.10}$$

The forward FFT corresponding to (2.10) is

$$X_k = \frac{1}{\sqrt{N}} \sum_{n=0}^{N-1} x_n \exp\left(\frac{-j2\pi kn}{N}\right), \text{ for } 0 \leq k \leq N-1 \tag{2.11}$$

The advantage of IFFT/FFT transform is that the discrete signal at the input and the receiver has the same total energy and same average power for each OFDM symbol.

1.4 Cyclic Prefix
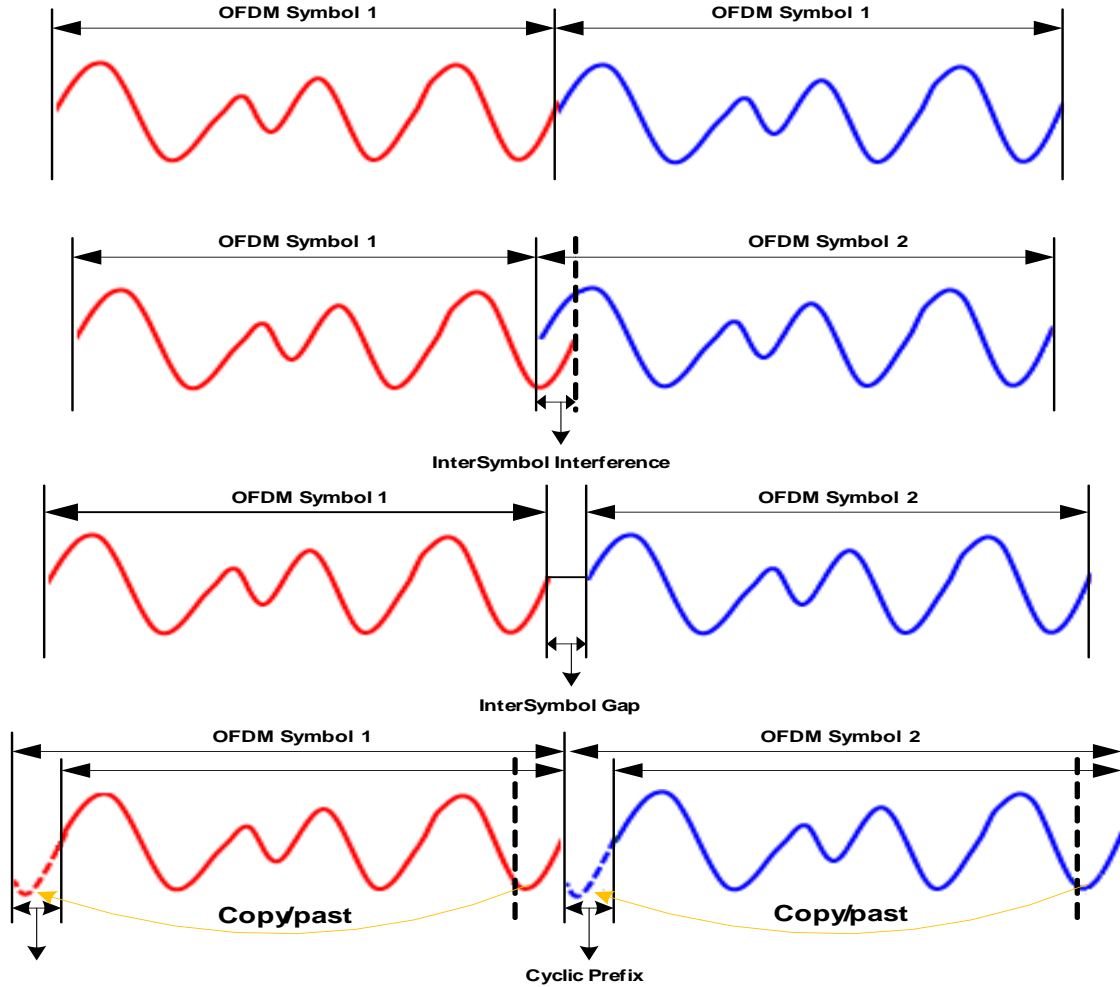
Figure 2.7: Steps of cyclic prefix generation

In order to eliminate the ISI and the ICI, the concept of cyclic prefix was propose [35]. Let's consider two consecutive OFDM symbols; Figure 2.7 shows the insertion of a cyclic prefix. As shown in figure 2.7, the waveform of the CP is an identical copy of the end of the same OFDM symbol. Section 2.3.4 shows how IFFT generates each OFDM symbol. A sequence of symbol will be transmitted. To denote different OFDM symbols, let extend the notation to add a time index. Therefore the output of the IFFT block in the ith OFDM symbol can be rewritten as a:

$$x(i) = [x_o(i)\,x_1(i)\,x_2(i).......x_{N-1}(i)]^T \tag{2.12}$$
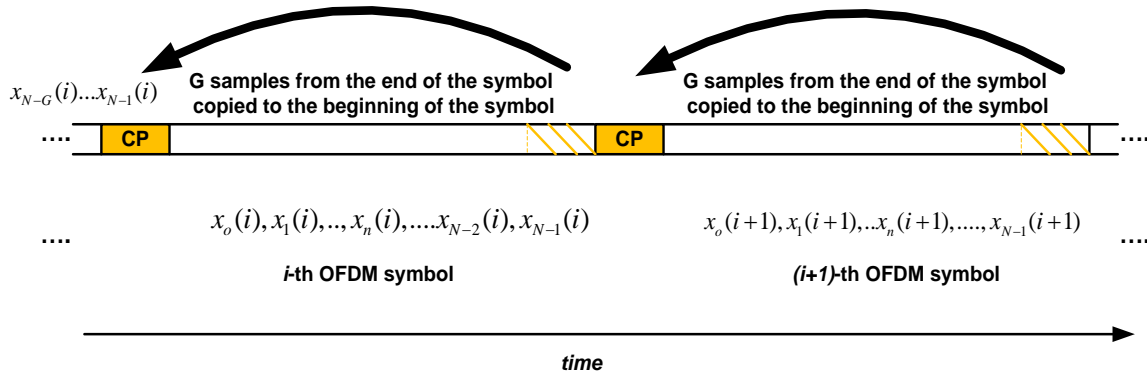
Figure 2.8: time domain sequence of OFDM symbols with CP

Figure 2.8 shows the time domain of *N* OFDM symbols with CP. Instead of transmitting the sequence $x(i) = [x_0(i)x_1(i)...x_{N-1}(i)]^T$, CP is added. G samples from the end of each symbol are copied to the beginning of the symbol and the sequence $x(i) = [x_{N-G}(i)..x_{N-1}(i),x_0(i)x_1(i)...x_{N-1}(i)]^T$ is transmitted.

1.5 DAC/ADC

In figure 2.5, it can be clearly seen that a DAC is required to convert the discrete value of sample to continuous analogue value, and an ADC needs to convert back the received signal to discrete sample.

2.2.3 Advantages of OFDM

OFDM is implemented in many emerging communications protocols because of its advantages over others traditional modulation techniques. Comparing with FDM, OFDM system has high spectral efficiency, reduces the inter-symbol interference and solves the multi-path distortion problem. The advantages of OFDM are: High spectral efficiency, resilience to multi-path distortion, reduced inter-symbol interference, efficient implementation using FFT, robust against narrow band co-channel interference, and low sensitivity against to time synchronization errors.

2.2.4 Majors drawbacks of OFDM

As well as known that OFDM has many advantages, it also has a number of drawbacks. The major drawbacks of OFDM systems are the high Peak-to-power average ratio (PAPR) and the sensitivity to phase noise and frequency offset

1. Peak-to-Average Power Ratio (PAPR)

Since OFDM has a multicarrier nature, the various subcarriers that make up the OFDM signal combine constructively. Consequently, since we are summing several sinusoids,

the OFDM signal in the time domain has a high PAPR. Because of this high PAPR, any transmitter nonlinearities would translate into out-of-band power and in-band distortion. Despite the OFDM signal having relatively infrequently occurring high peaks, these peaks can still cause sufficient out-of-band power when there is saturation of the output power amplifier or when there is even the slightest amplifier non-linearity [36]. Figure 2.9 shows high peaks generations by adding four sinusoidal with different frequencies and phase shifts.
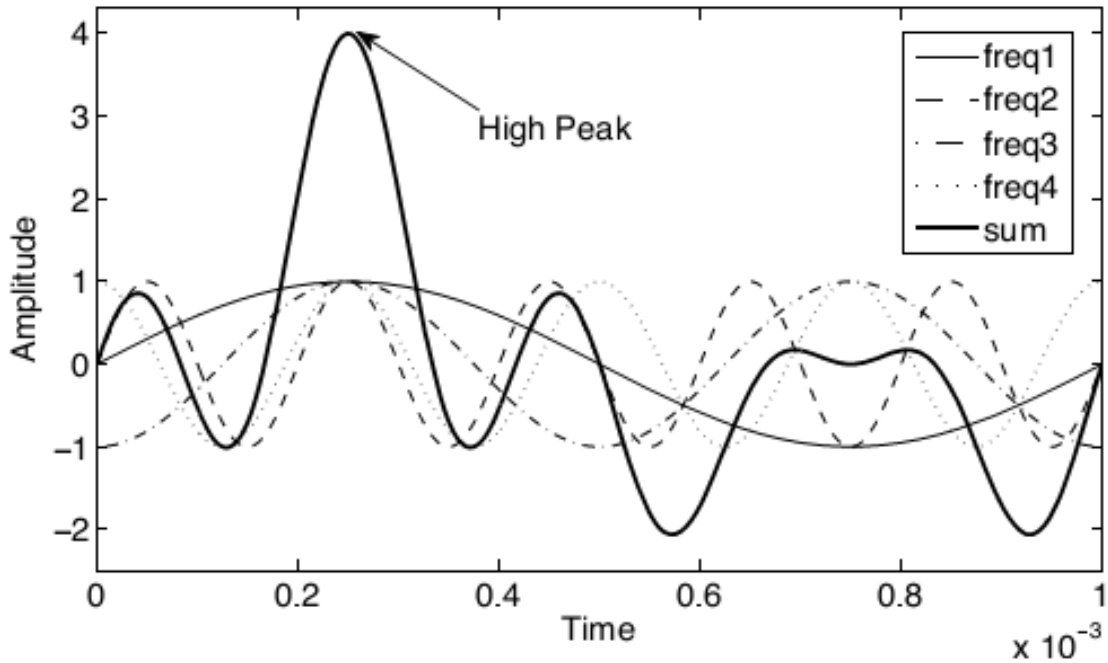
Figure 2.9: High peaks generated by summing four sinusoids

For a given OFDM signal $x(t)$ defined above where N subcarriers are added. If N is large, the samples of the OFDM signal have approximately Gaussian distributions according to the central limit theorem (CLT) [32].

The PAPR can be defined as the ratio of the maximum instantaneous power to the average power:

$$PAPR = \max_{0 \le n \le N-1} \frac{|x(t)|^2}{E[|x(t)|^2]} \tag{2.13}$$

where $E[.]$ is the expectative operator. In wireless communication, the high PAPR will produce signal excursions into nonlinear region of power amplifier (PA) at the transmitter level which leads to nonlinear distortions and spectral spreading [37]. In optical communications, EDFAs are employed. These amplifiers are characterized by a

slow response time, making them linear regardless of the input signal power. Nevertheless, the high PAPR of OFDM is still a challenge because of the non-linearity of the external modulator, the ADC and the optical fiber [3] when the OFDM signal is transmitted over fiber. The statistics for the PAPR of an OFDM signal can be given in terms of its complementary cumulative distribution function (CCDF). The CCDF of PAPR is defined as the probability that the PAPR of the OFDM symbols exceeds a given threshold PAPR0. The CCDF for an OFDM signal is expressed as

$$CCDF = P(PAPR>PAPR0) \qquad (2.14)$$

In wireless communication, high PAPR drives the PA into saturation which leads to BER performance degradation and spectrum corruption. In optical fiber communication, if PAPR is high, the nonlinear effect of the Mach–Zehnder modulator (MZM) and digital-to-analog converter/analog-to-digital converter (DAC/ADC) will also introduce nonlinear distortion. To solve these problems, the PAPR needs to be reduced. Many techniques have been proposed. These techniques can be divided into two groups: The first group intends to reduce the occurrence of large signals before multicarrier modulation, the second group processes the OFDM signals directly.

1.1 Reduction the occurrence of large signals

The well know techniques of this group are: Selective mapping (SLM) [38, 39], partial transmit sequence (PTS) [40-42], spreading code [43, 44], dummy sequence insertion (DSI) [45], pre-code [46, 47], coding [48-50], active constellation extension (ACE) [51], Tone Reservation [52]...

1.2 Process the OFDM signals directly

The well know techniques of this group are: conventional clipping and filtering [37, 53], Bayesian clipping recovery [54], companding [55-58], peak windowing [59] and peak cancellations [60]...

A novel new hybrid method PAPR reduction technique based on carrier interferometry codes combined with companding technique and a novel new binary particle swarm (NBPSO) based on DSI method have proposed in this thesis. Detailed discussions are offered in chapter 4 and chapter 5, respectively.

2. Frequency Offset and Phase Noise

In OFDM, information is transmitted over orthogonal subcarriers in each OFDM symbol. The differences in the frequency and the phase of the receiver local oscillator

and the carrier of the received signal can result in system degradation. These impairments are usually classified in terms of their, for example, frequency offset between transmitter and receiver local oscillator [61], Doppler spread in channel [62],and variety of phase models with characteristics that depend on the mechanisms of carrier recovery at the receiver [63, 64].

2.3 Optical OFDM

The principle of Optical OFDM system has been briefly introduced in section (1.1). This section will focuses on the Optical OFDM system from its different components to its two major variants: Coherent Optical OFDM and IM/DD optical OFDM.

After that, a comparison will be made between these two techniques of detection in order to present their advantages and disadvantages.

2.3.1 Key optical components

This section describes the basic optical components used in an optical transmission system. Figure 2.10 shows the end-to-end optical transmission involves both electrical and optical signal paths. To perform conversion from electrical to optical domain, the optical transmitters are used, whereas to perform conversion in the opposite direction (optical to electrical conversion), the optical receivers are used. The optical fibers serve as the foundation of an optical transmission system because they are used as a medium to transport the optical signals from source to destination. As we know, the optical fiber attenuates the optical signal during the transmission, to restore the signal quality, optical amplifiers such as, Erbium-doped fiber amplifiers (EDFAs), have to be used. To impose the information signal, optical modulators are used. The optical modulators are commonly used in combination with semiconductor lasers. The main purpose of the optical receiver, terminating the light-wave path, is to convert the signal coming from fiber from optical to electrical domain and process appropriately such obtained electrical signal to recover the data being transmitted. The optical signal is converted into electrical domain by using a photo-detector.
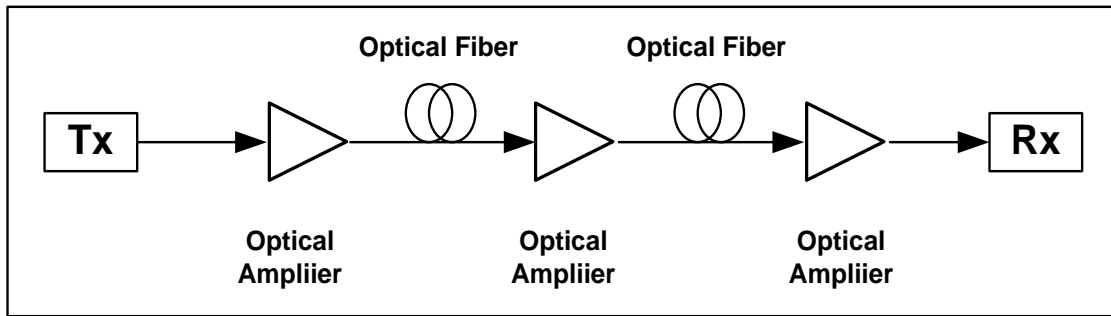
Figure 2.10: Typical optical transmission Link

1. Optical transmitters

The main roles of the optical transmitters are to generate the optical signal (generally via an semiconductor laser) and launch the modulated signal into the optical fiber. It can be done by external modulation or direct modulation. The direct modulation of semiconductor lasers lead to frequency chirp. For high transmission data rates, external modulation provides a better optical modulation solution than direct modulation. This is because as data rates increase, the bit durations become smaller and the impact of the pulse broadening caused by laser chirp becomes more severe. The external modulator used for all experiments in this thesis. The external modulation includes commonly semiconductor lasers and Mach–Zehnder modulator (MZM), whereas the semiconductor lasers are biased by a dc voltage to produce a continuous wave operation.

1.1 Semiconductor lasers

Light amplification by stimulated emission of radiation (Laser) produces high powered beam of coherent light which contains distinct frequencies. Generally, they are three main types of laser used in optical communication.

> ➤ Distributed Feedback Laser (DFB): these kinds of lasers operates at longer wavelength (1310 or 1550 nm windows). They are high cost and edge emitters.

> ➤ Vertical Cavity Surface Emitting Laser (VCSEL): these laser are predominantly multi transversal mode and low cost. They operate at 850 nm.

> ➤ Fabry Perot Laser (FP): they operate at longer wavelength (1310 or 1550 nm windows) with multiple longitudinal modes. They are edge-emitters and moderated cost between VCSEL and DFB lasers.

1.2 Mach-Zehnder modulator

A typical dual-electrode MZM (DE-MZM), as shown schematically in Figure 2.11, is made of Lithium Niobate (LiNbO$_3$) and comprises two Y-junctions. Light in the waveguide on getting to the first Y-junction is split into two halves. The electro-optical properties of enable a phase modulation of the light in both arms depending on whether or not an electrical field is applied to the electrodes. With no electrical field applied, there is no phase difference between the two arms and the light combines to give an intensity maximum at the output of the DE-MZM. An application of an electrical field results in a phase difference, which could result in constructive or destructive interference. Let $V_1(t)$ and $V_2(t)$ denote the electrical drive signals on the upper and lower electrodes, respectively. If the phase difference is π, there's total destructive interference, corresponding to the "off" state for the DE-MZM. An MZM where only one of the arms is modulated with a voltage is referred to as a single-electrode MZM. With an ideal extinction ratio assumed, and ignoring the insertion loss of the MZM; if the D.C. offset voltage at which maximum transmission is obtained is assumed to be 0, the output electrical field $E_{out}(t)$ of the second Y-branch can be related to the input optical field $E_{in}(t)$ by [3, 65]
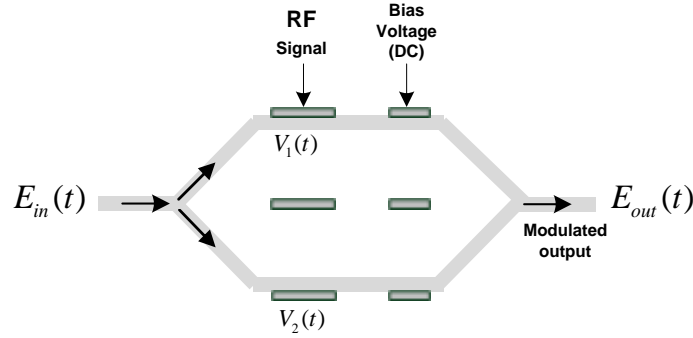
Figure 2.11: Mach-Zehnder modulator

$$E_{out}(t) = \frac{1}{2}\left[\exp\left(j\frac{\pi}{V_\pi}V_1(t)\right) + \exp\left(j\frac{\pi}{V_\pi}V_2(t)\right)\right]E_{in}(t) \qquad (2.15)$$

where $V\pi$ is the half-wave voltage (the voltage at which there's complete suppression of the MZM output $V\pi = V_1 - V_2$).

If a DC bias voltage is applied to one of the electrodes of the MZM while the other DC terminal is grounded. The output electrical field $E_{out}(t)$ can be as [65]:

$$E_{out}(t) = \frac{B}{2}\left\{\left\{\sum_{n=-\infty}^{\infty} J_n\, e^{j\left((\omega_c + n\omega_{RF})t + \frac{n\theta}{2}\right)}\left(e^{j\frac{n\theta}{2}} + e^{j\left(\varepsilon\pi - \frac{n\theta}{2}\right)}\right)\right\}\right\} \tag{2.16}$$

where $J_n(x)$ is the Bessel function of the first kind of order n, $\varepsilon = V_{DC}/V_{\pi}$, θ is the phase angle of the RF signal, ω_{RF} is angular frequency of RF signal, ω_c is center angular emission frequency of input optical field (Semiconductor lasers).Equation (2.8) indicates that the optical signal at the output of the MZM is also a DSB-C signal, made up of the optical carrier at the laser center emission frequencyω_c, and several sidebands, located at multiples of the frequency of the modulating RF signal ω_{RF}. Depending on the value of the DC bias voltage, we can end up suppressing the optical carrier and the even-order optical sidebands, or the odd-order optical sidebands. To generate the DSB-C signal, the two arms of the MZM are driven by two RF signals with equal amplitude but out of phase by π.

2. Optical fibers

Optical fibers serve as the foundation of an optical transmission system because they transport optical signals from source to destination. The combination of low-loss and extremely large bandwidth allows high-speed signals to be transmitted over long distances before the regeneration becomes necessary. According to [68], optical fiber has three-low attenuation regions. The first one is centered at 800 nm with an attenuation of 2.5 dB/Km, the second region is centered at 1300 nm with an attenuation of 0.5 dB/Km, and the third region is centered at 1550 nm with an attenuation as low as 0.2 dB/Km. The available bandwidth can be measured in terms of either wavelength or frequency by using the equation:

$$\Delta f \approx \frac{\Delta\lambda.c}{\lambda^2} \tag{2.17}$$

where *c* is the speed of light, is the corresponding wavelength, and Δf, and $\Delta\lambda$ represent the bandwidth expressed in terms of frequency and wavelength respectively. Considering the 1300 and 1550 nm transmission windows, and taking the usable bandwidth in these bands to be the bandwidth over which the loss in dB/km is within a factor of 2 of its minimum, from (2.9) the available usable bandwidth is about 35 THz. According to the mode of propagation in the fiber, generally two types of fiber can be defined: single mode fiber (SMF) and multimode fiber (MMF). Figure 2.12 shows a comparison of single mode fiber and multimode fiber.
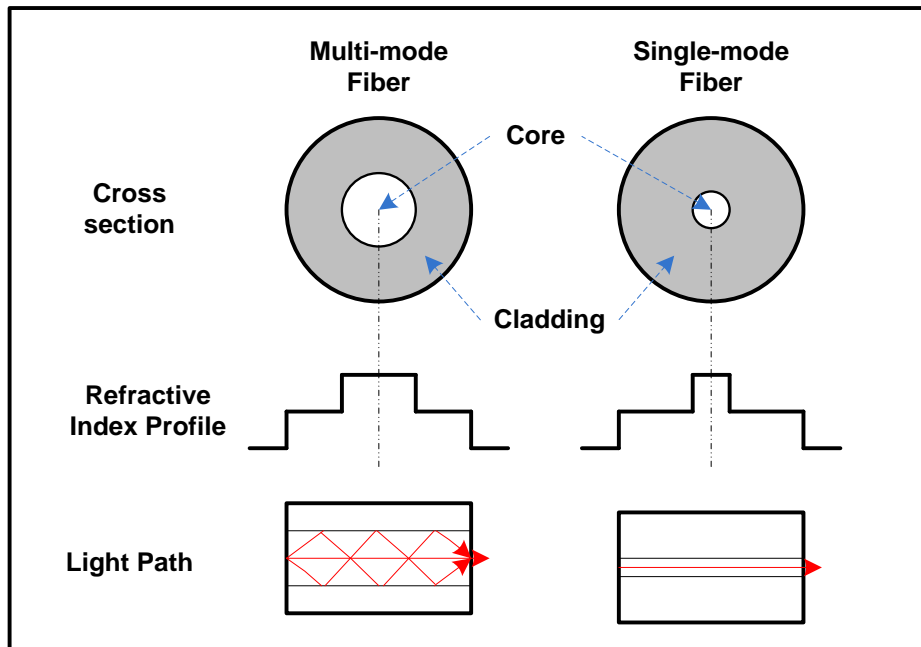
Figure 2.12: Multi-Mode Fiber versus Single Mode Fiber

If more than one mode propagates through a fiber, it called multimode. The advantages of multimode fiber is that its core is large; as a results, the injection of light through the fiber can done using inexpensive light sources such as light-emitting diodes (LED). It major disadvantage is that multimode fiber introduces the phenomenon of intermodal dispersion.

In single mode fiber just one mode is allowed to be transmitted through the fiber. SMF eliminates intermodal dispersion and can support transmission over longer distances. With the fact that its core is very small, the use of semiconductor laser is needed to generate high concentration light energy to be transmitted through the fiber with long distance.

3. Optical amplifiers

The purpose of optical amplifier is to restore the signal power level without any conversion (electric to optic or optic to electric). As we know the optical signal suffers signal degradation when propagated over some distance. Figure 2.13 shows the general form of an optical amplifier.

Optical amplifiers use the principle of stimulated emission. The amplification gain G can be defined as a ratio of the output power P_{out} by the input power P_{in} of the optical amplifier medium $G=P_{out}/P_{in}$. There are two basic types of amplifier such as semiconductor laser amplifier and doped-fiber amplifiers in which the most doping

element is erbium. Now, the Erbium-Doped Fiber Amplifiers are widely used. Conventional EDFAs typically operate in the 1530 to 1570 nm frequency band. Substituting Δλ=40 nm in (2.9) yields a usable bandwidth of around 5 THz.
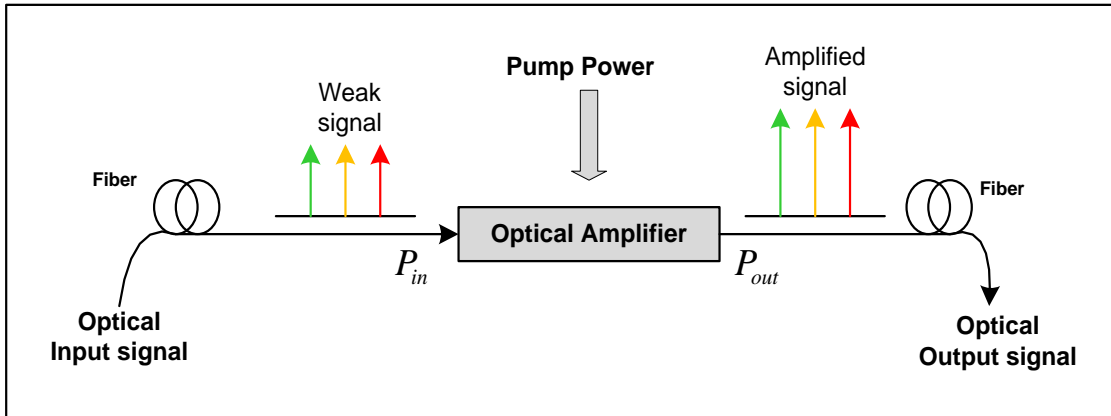
Figure 2.13: Principle of optical Amplifier

4. Photo-detector receivers

The purpose of optical receivers is to convert back the optical signal in an electrical form and to recover the transmitted data.

The basic direct detection device in optical communication network is the photodiode. The photodiode absorb photons in incoming optical signal and convert them back to the electrical signal. The common photodiodes can be divides into five classes: p-i-n photodiodes, p-n photodiodes, avalanche photodiodes (APD) and metal-semiconductor-metal photodiodes (MSM). The p-n photodiode consists of a reverse-biased p-n junction. The p-i-n photodiode is based on an intrinsic region between p and n junction. The APD is a modified p-i-n photodiode that is operated in a very high reverse bias.

5. Channel Impairments

This section describes different channel impairments, including fiber attenuation, insertion losses, chromatic dispersion, PMD, and fiber nonlinearities.

1.1 Fiber Attenuation

Attenuation in optical fiber is a degradation of the signal power as the signal propagates over some distance. It can be described by the general relation dP/dz=αP, where α is the power attenuation coefficient per unit length (dB/km). Let consider an optical fiber with L-km of length, the received optical power P_{out} after L-km propagation can be characterized as:

$$P_{out} = P_{in} \exp(-\alpha L) \tag{2.18}$$

where P_{in} is power launched in to fiber.

1.2 Chromatic Dispersion

Chromatic Dispersion can be defined as the wavelength dependent pulse spreading that occurs as the optical signal propagates through the fiber. Two factors contribute to the chromatic dispersion such as the waveguide dispersion and the dependence of the fiber material's refractive index on the wavelength.

The pulse spreading due to chromatic dispersion can be given by:

$$\Delta t = D(\lambda).\Delta\lambda.L \tag{2.19}$$

where $D(\lambda)$ (ps/nm/Km) is the dispersion parameter, $\Delta\lambda$ is the spectral width of the light source, L is the optical fiber length.

The dispersion parameter $D(\lambda)$ is approximated by[66]as:

$$D(\lambda) = \frac{S_o}{4}\left[\lambda - \frac{\lambda_0^4}{\lambda^3} \right] \tag{2.20}$$

where S_o is the zero dispersion, is slope and λ_0 is the zero-dispersion wavelength.

2.3.2 IM/DD Optical OFDM

Figure 2.14 shows the basic diagram of an IM/DD optical OFDM system [67]. The system can be divided into five parts including the OFDM transmitter, the electrical-to-optical up conversion, the optical fiber link, the optical-to-electrical down conversion and the OFDM receiver.

1. OFDM transmitter

A streaming data is sent to the transmitter; due to the intensity modulator used for OE up conversion, real valued OFDM signals is needed to drive the MZM modulator. To produce a real value OFDM, the Hermitian symmetry has to be imposed on the OFDM frame before the IFFT operation. The Hermitian symmetry can be expressed as:

$$Xk = \begin{cases} 0 & k = 0 \\ X_k & k = 1,...., N/2-1 \\ 0 & k = N/2 \\ X_{N-K}^* & k = N/2+1,....., N-1 \end{cases} \tag{2.21}$$

An IFFT is then applied to each subcarrier to generate N parallels real value symbols before being converted into serial stream data. After CP insertion, the signal is converted into an analogue form and achieved as EO up- conversion.
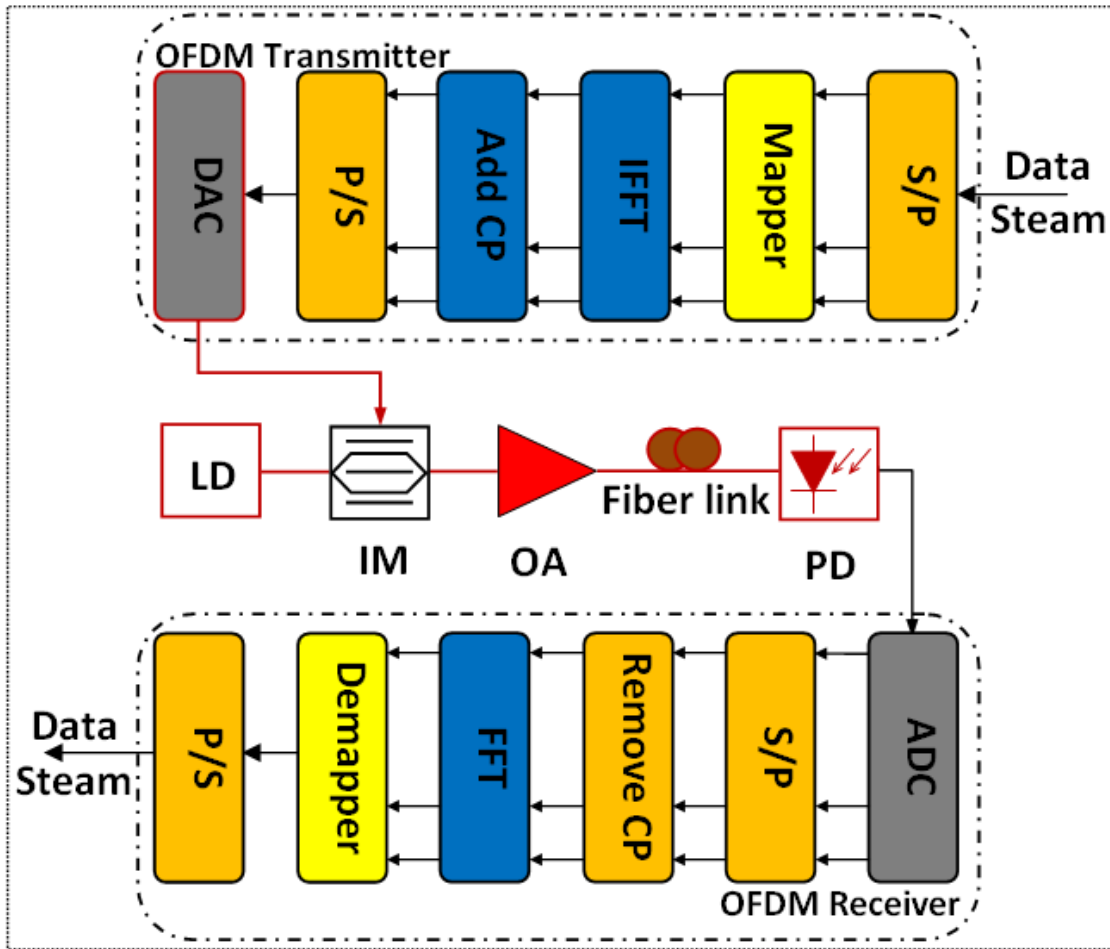
Figure 2.14: Conceptual diagram of IM/DD optical OFDM system

2. Electrical-to-Optical up conversion

MZM is used as intensity modulator to transfer the OFDM signal from electrical domain to optical domain to create an optical OFDM signal.

3. Optical fiber link

Optical fiber link is the medium of transmission. When the optical OFDM system launches an optical signal into the optical fiber, after some distance of transmission the optical signal is degraded and an optical amplifier is needed to compensate for the link loss.

4. Optical-to-Electrical down conversion

At the OE stage, the optical OFDM signal is directly detected using a photodiode.

5. OFDM receiver

In the OFDM receiver, after passing through the ADC, the electrical signal is converted into original data sequence by the receiver which is the inverse of the transmitter.

2.3.3 Coherent optical OFDM

Figure 2.15 shows a typical Coherent optical OFDM system which includes five basic functional blocks: OFDM transmitter, the electrical-to-optical up conversion, the optical fiber link, the optical-to-electrical down conversion and the OFDM receiver [36].
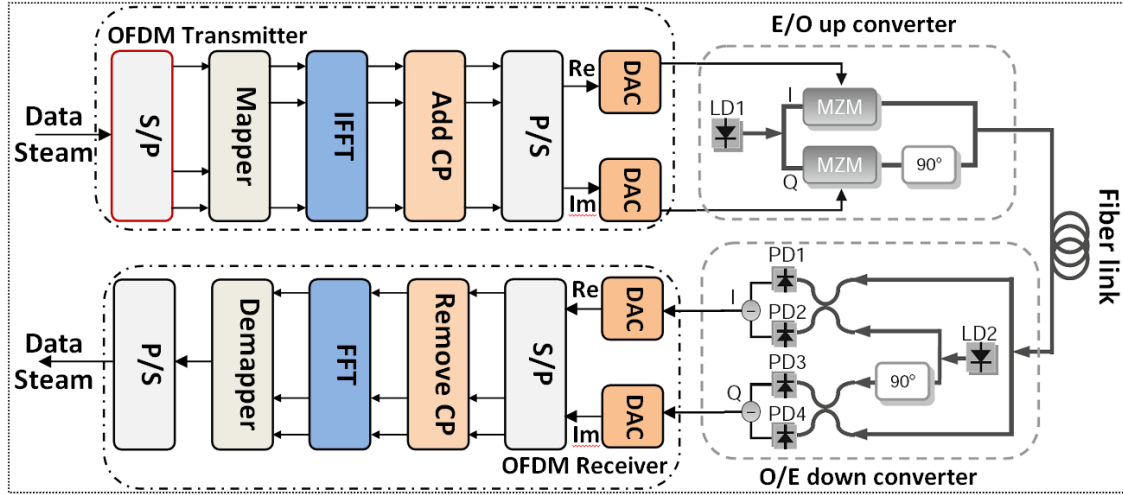
Figure 2.15: Conceptual diagram of Coherent optical OFDM system

Compared with the IM/DD optical OFDM system, the coherent detection optical OFDM needs to transfer a complex baseband OFDM signal. The EO up-converter converts the complex baseband OFDM signal into optical domain using I/Q modulator composed of a pair of MZMs with 90° phase offset. The converted baseband OFDM signal after the EO up-conversion can be given by

$$E_{out1}(t) = x(t)\exp(j\omega_{LD1} + \varphi_{LD1})$$
(2.22)

where ω_{LD1} and φ_{LD1} are the angular frequency and the phase of the transmitter laser respectively. Then, the baseband optical OFDM signal passes through the optical fiber with impulse response $h(t)$. The received optical signal after some distance of transmission can be defined as:

$$E_{receiv}(t) = [x(t)\exp(j\omega_{LD1} + \varphi_{LD1})] \otimes h(t)$$
(2.23)

where $\otimes$ is the convolution operator. The received signal is then sent into the OE down-converter to be converted into an electrical form. The down converted signal can be expressed as:

$$E_{DC}(t) = \left\{ x(t)\exp[j(\omega_{LD1}+\omega_{LD2})+(\varphi_{LD1}-\varphi_{LD2}) \right\} \otimes h(t) \qquad (2.24)$$

where (ω_{LD1} - ω_{LD2}) and (φ_{LD1} - φ_{LD2}) are the frequency offset and the phase offset between the transmitter and the receiver lasers respectively.

At the receiver, the down-converted OFDM signal is sampled with two ADCs before processing with the receiver which is the inverse of the transmitter.

2.3.4 IM/DD OOFDM versus Coherent OOFDM

After discussing the principle of IM/DD optical OFDM system and coherent optical OFDM, a brief comparison between these two systems will be made. Table 2.1 shows the differences of the two systems in the following points: Modulation technique, detection technique, OFDM signals value, complexity and applications.

Table 2.1: IM/DD optical OFDM versus Coherent optical OFDM

	IM/DD optical OFDM	Coherent optical OFDM
Modulation	Intensity Modulator	Optical I/Q modulator
Detection	Square law direct detection	Coherent detection with local oscillator
OFDM Signal value	Real	complex
Complexity	Low	High
Application	MANs, LAN, Access networks	Long haul core networks

2.4 Summary

In this chapter, the optical OFDM basics are presented for a better understanding of the rest of the thesis. A review of the historical perspectives of OFDM and its applications are given. After that the basic concept of OFDM transceivers are explained including, serial-to-parallel and parallel-to-serial, mapping and de-mapping, IFFT/FFT, cyclic prefix and DAC/ADC converters. The advantages and disadvantages of OFDM are described with some techniques to overcome the main drawback of the OFDM signal such as the PAPR. On the others hand, the key components of optical transmission link,

optical lasers transmitter, optical modulator, optical fiber, optical amplifier and the photo-detector receivers, are presented and discussed. Finally, the two major models of optical OFDM system: IM/DD Optical OFDM and Coherent Optical OFDM have been detailed and compared.

Chapter 3: **A PAPR REDUCTION SCHEME BASED ON A NEW SPREADING CODE**

3.1 Introduction

Due to its ability to combat transmission impairments and its high spectral efficiency, orthogonal Frequency Division Multiplexing applied in optical communication such as optical OFDM has interested many researchers [68]. Generally speaking there are two major variants of Optical OFDM according to the configuration of the receiver: intensity modulator and direct detect (IM/DD) optical OFDM [10] and coherent detection optical OFDM [8]. A number of researchers have found that IM/DD optical OOFDM is a promising technology for cost sensitive MANs, Access network and LAN [69] because of it simple configuration, low complexity and its higher tolerance to the fiber chromatic dispersion (CD) [70] and polarization mode dispersion (PMD) [71]. IM/DD configuration is advantageous because of its simple receiver configuration which needs only one photodiode to convert back the optical signal to electrical signal. Comparing to Direct Detection system, the coherent optical OFDM has better sensitivity and spectral efficiency. In the coherent detection, an optical local oscillator, 90° optical hybrids, the high-speed analog/digital convertor and the digital signal processing [72] are needed. These devices increase the complexity and the cost of the system [73, 74].

IM/DD Optical OFDM system is cost effective because of the simple receiver configuration. However, OFDM is not perfect for IM/DD optical OFDM; the main drawback of OFDM is it high PAPR. When the optical launch power into the optical fiber is very high, high PAPR causes nonlinear effects in the fiber transmission. Therefore, PAPR reduction techniques become an important challenge in IM/DD optical OFDM transmission systems in order to increase their tolerance to optical intensity modulator, digital-to-analog/analog-to-digital convertor (DAC/ADC) and fiber nonlinearity [40, 75]. To reduce the PAPR in optical OFDM systems, various approaches have been proposed such as Partial Transmission Sequence (PTS) [41], Selective Mapping (SLM) [39], coding schemes [48], conventional clipping and filtering based on FFT/IFFT [37, 53], Bayesian clipping recovery [54], nonlinear companding transforms [76], Hadamard transform [77], The Carrier Interferometry codes (CI) [43]. All These techniques can be used to reduce PAPR, but there are some disadvantages.

Conventional clipping causes both in-band distortion and out-of-band distortion, and further it causes an increasing of system's bit error rate. The Bayesian clipping recovery scheme can be enhanced the system performance in both the error rate and complexity. The scheme utilizes a priori information about the sparsity rate and noise variance to improve the system performance, however, it has side information. The companding techniques have better performance than conventional clipping schemes, however, it does not make the envelope of the OFDM signal constant due to the limitation of the BER [56]. The drawbacks of SLM and PTS are high computational complexity and bandwidth expansion. The CI code [43] is one kind of spreading code, it can significantly improve BER performance. But CI just results in reordered original data, and it is not capable of supporting user.

To reduce the nonlinear distortion in electrical and optical devices and transmission fiber, we propose and experimentally demonstrate a peak to average power ratio (PAPR) reduction scheme based on new spreading code in direct detection optical OFDM system. The new spreading code [44] with high auto-correlation and low cross correlation while is able to capable of supporting $2N+1$ users. That means, $2N+1$ users or data symbols can be transmitted over only N sub-carriers. Therefore, it can save the bandwidth.

Our experimental results show that new spreading code is able to provide better performance in terms of both PAPR reduction and BER for OFDM systems.

This chapter is organized as follows: Section 3.2 describes the principle of new spreading code. Then, we introduce the experimental setup and results in Section 3.3. Finally, the concluding remarks are given in Section 3.4.

3.2 Principle of new spreading code

3.2.1 OFDM transmitter with new spreading code

In traditional OFDM each data symbol is modulated onto its own subcarrier and sent over the channel. Here, in new spreading OFDM system, each data symbol is multiplied by spreading code $C(k,n)$ and then spreads out onto all of the subcarriers as shown in Figure 3.1, where n is the subcarrier index and k is data index (or symbol-k) of new spreading OFDM system.
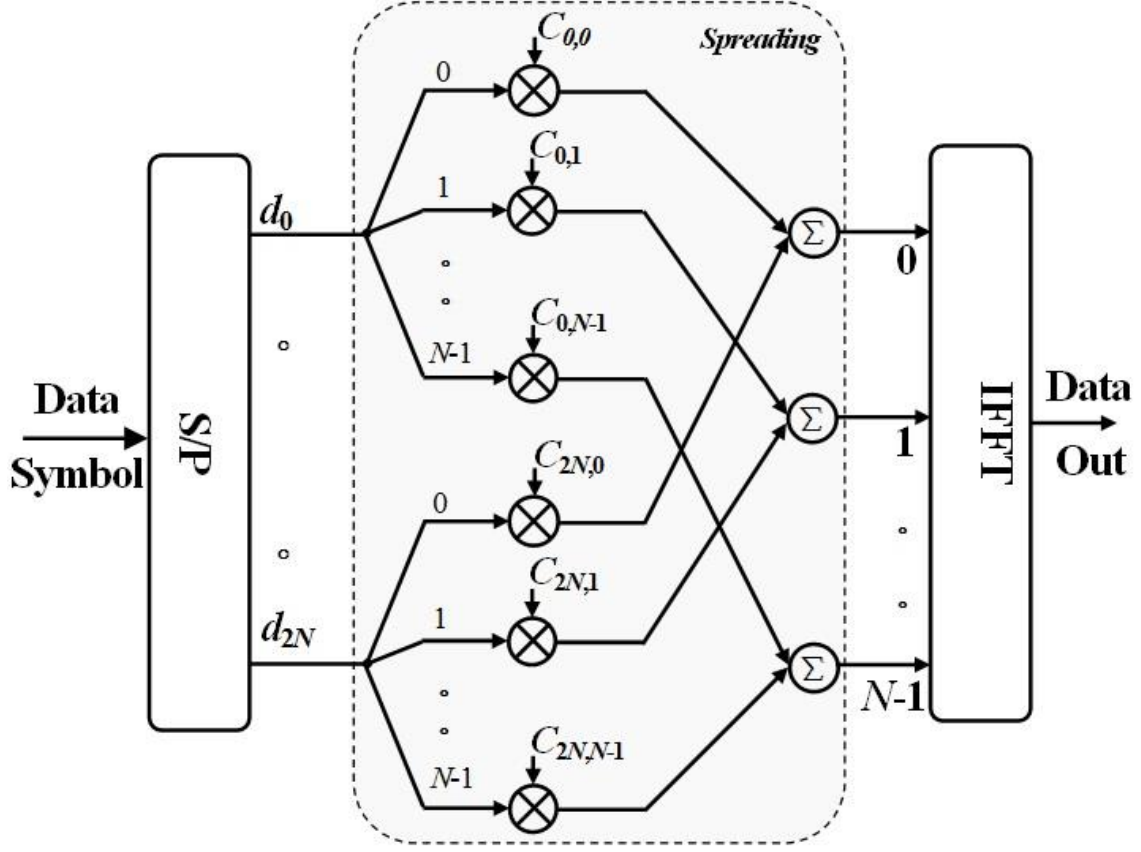
Figure 3.1:The transmitter of OFDM system with new spreading code

In traditional OFDM system, the base-band OFDM signal is given as:

$$X(t) = \frac{1}{\sqrt{N}} \sum_{k=0}^{N-1} \sum_{i=0}^{N-1} d^{(k)} e^{j(2\pi i \Delta ft)}, \tag{3.1}$$

where d is the data symbol, Δf is the carrier spacing of IFFT, and N is the number of subcarriers.

The signal of new spreading code for real data ($d=\{-1,1\}$) can be expressed as:

$$S(t) = \frac{1}{\sqrt{N}} \sum_{k=0}^{K-1} \sum_{i=0}^{N-1} d^{(k)} e^{j(2\pi i \Delta ft)} C_{(k,i)}, \tag{3.2}$$

where $C(k,i)$ are coefficients of new spreading code, where $K=2N+1$, and $C_{(k,n)}$ structure for N sub-carriers are written by

$$C_{(k,n)} = e^{j\left(\frac{2\pi}{2N+1}\right)k(2n+1)}, \text{ for } \begin{array}{l} n = 0,1,..,N-1 \\ k = 0,1,..,2N \end{array} \tag{3.3}$$

With CI codes [43], where $K=N$, and $C(k,n)$ structures for N subcarriers are written by:

$$C_{(k,n)} = e^{j\left(\frac{2\pi}{N}\right)kn}, \text{ for } \begin{array}{l} n = 0,1,..,N-1 \\ k = 0,1,..,N-1 \end{array} \qquad (3.4)$$

It can be seen from Eq. (3.3) that, new spreading code is able to capable of supporting $2N+1$ symbols or $2N+1$ users used number of sub-carriers is N. It can save the bandwidth.

The PAPR of the OFDM signal with new spreading code can be expressed as:

$$PAPR = \frac{\max |S(t)|^2}{E\{|S(t)|^2\}}, \qquad (3.5)$$

where $E\{\cdot\}$ denotes the expectation. $E\{|S(t)|^2\}$ is equal to the variance σ^2, since the symbols are zero mean. The statistics for the PAPR of an OFDM signal can be given in terms of its complementary cumulative distribution function (CCDF). The CCDF of PAPR is defined as the probability that the PAPR of the OFDM symbols exceeds a given threshold $PAPR_0$. The CCDF for an OFDM signal can be written as

$$CCDF = P(PAPR > PAPR_0) \qquad (3.6)$$

3.2.2 OFDM receiver with new spreading code

Figure 3.2 shows the receiver of OFDM system with new spreading code.
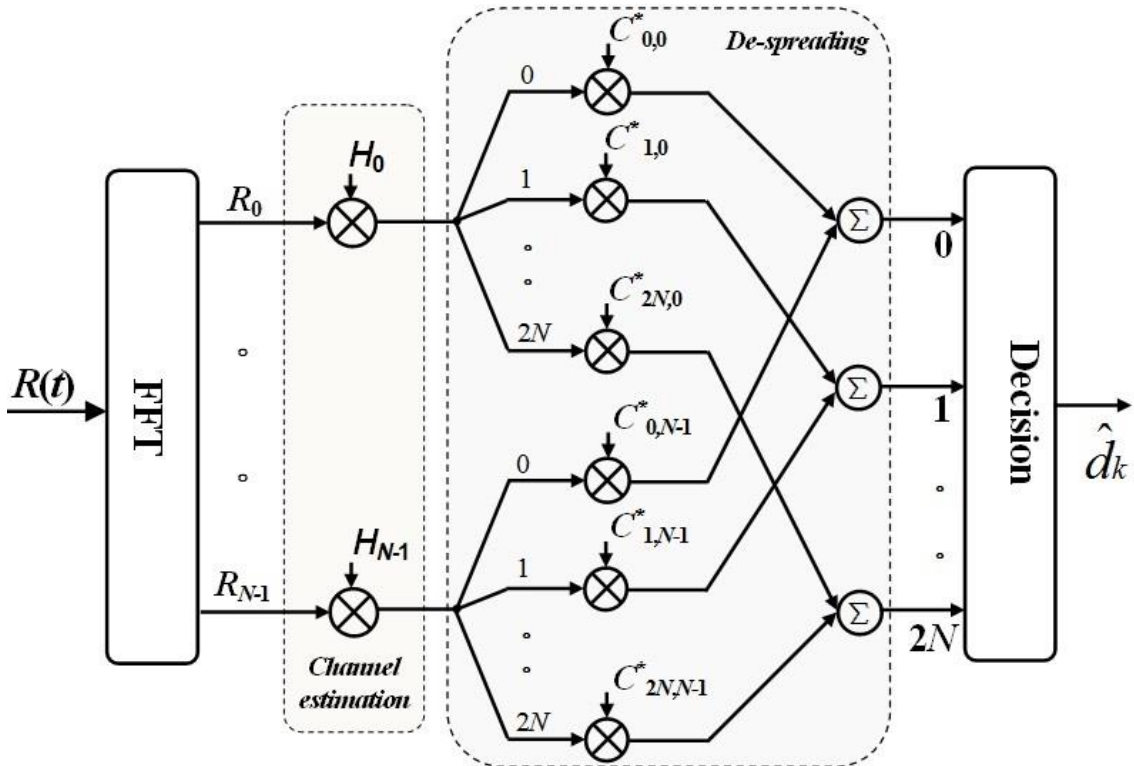
Figure 3.2: The receiver of OFDM system with new spreading code

The received signal $R(t)$ from the channel passes through the FFT module to obtain the frequency domain signal, which is then equalized with coefficient H_i. The equalized signals are then de-spread with complex conjugate codes $C^*_{(k,n)}$. Finally, the hard decision device is employed to create a final decision of $\hat{d}_k$.

In this experiment, the channel estimation and the synchronization symbol are realized by using training sequence (TS).

The basic form of proposed TS is similar to Park's method [78]. The synchronization symbol is realized by Chen's method [79], only the sign bit of ADC captured sample is extracted to realize the synchronization with simple XNOR and bit summation operations. The timing metric is defined as:

$$M(d) = \begin{cases} P(d) + P(d-1), & \text{if } P(d) > V \\ P(d), & \text{if } P(d) \le V \end{cases} \tag{3.7}$$

where

$$P(d) = 2 \sum_{n=0}^{N_t-1} sign[t(n)] \odot sign[r(n+d)] - N_t \tag{3.8}$$

where t(n) is the transmitted training sequence of length $N_t = N + N_{cp}$, N is the size of IFFT, N_{cp} is the length of cyclic prefix, $r(n)$ is the received signal, sign[.] stands for sign bit extractor, as the input is a positive number, the output is bit '0'; otherwise the output is bit '1'. $\odot$ is the XNOR operator, V is a threshold value.

The channel estimation is calculated as Chen's method [80]. The channel information on the even subcarriers can be estimated from the two adjacent odd subcarriers through frequency-domain interpolation. The even channel response can be obtained by linear interpolation

$$H_{\text{even}}(i) = \frac{H_{\text{odd}}(i-1) + H_{\text{odd}}(i+1)}{2}, \tag{3.9}$$

where $H_{\text{even}}(i)$ denotes the channel response on the ith sub-carrier with even index, $H_{\text{odd}}(i\text{-}1)$ and $H_{\text{odd}}(i+1)$ are the channel response for two adjacent odd subcarriers.

3.3 Experimental setup and results

3.3.1 Experimental setup

Figure 3.3 describes the experimental setup of the IM/DD optical OFDM transmission system. There are four signals in this experiment. Signal of new spreading code is BPSK modulated, signal of CI codes and origin are 4QAM modulated. The parameters of the experiment setup are shown in Table 1.
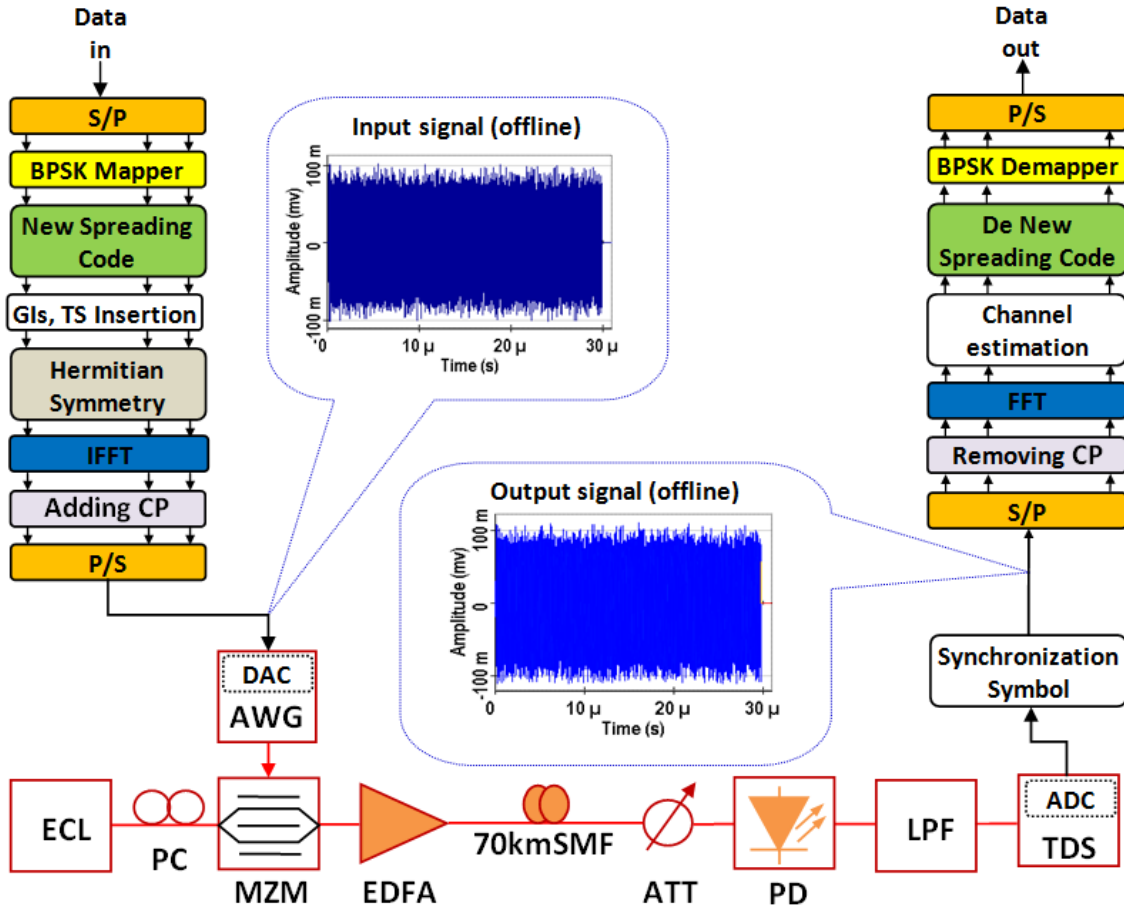
Figure 3.3: The experimental setup for the IM-DD OOFDM transmission system with OFDM signals. ECL: external cavity laser, ATT: attenuator, PC: polarization controller, DAC: digital to analog converter, AWG: arbitrary waveform generator, MZM: Mach–Zehnder modulator, EDFA: erbium doped fiber amplifier, PD: photodiode, LPF: low pass filter, and TDS: real-time digital storage oscilloscope, ADC: analog to digital converter.

The pseudo-random binary sequences (prbs) are converted into parallel data by S/P converter (the number of parallel signals is 393 for new spreading-OFDM with 512 subcarriers, 201 for new spreading-OFDM with 256 subcarriers, and 100 for CI-OFDM and original OFDM, respectively). The parallel data is mapped into a BPSK modulation for new spreading code, 4QAM modulation for CI code and original OFDM, then

spread by spreading phase codes $C_{(k,n)}$ (detailed in Section 2.1). After that add GI and Hermitain constrains, and then passed through an IFFT block. The IFFT produces a complex-valued time domain waveform. After IFFT, the CP is added to mitigate the ISI.

Table 3.1: The parameters of experiment

Items	Sub items	Value
OFDM (CI and Original OFDM)	FFT size	256
	Sub-carriers for data	200
	CP	32
	The length of prbs	51200
	Modulation	4QAM
	OFDM symbol	256
OFDM (New spreading)	FFT size	256/512
	Sub-carriers for data	200/392
	CP	32/64
	Null sub-carriers	56/110
	Modulation	BPSK
	The length of prbs	51456/100608
	OFDM symbol	256
Training sequence (TS)	Training sequence	1
MZM	Bias voltage (V)	2.4
	Power output (dBm)	-2
Fiber	Fiber length (km)	70km
	Attenuation (dB/km)	0.19
	Dispersion (ps/nm/km)	16.75
	Dispersion slope (ps/nm^2/km)	0.075
	Effective area (um^2)	80
	n_2 (m^2/w)	2.6e-20
	SNR (dB)	15
AWG (AWG710)	DC bias(V)	2
	Sample rate (Gsample/s)	2.5
PD (83446A)	Wavelength Range (nm)	1200 to 1600
	Auxiliary Out Bandwidth(MHz)	0.1 to 1500
ECL	Power output (dBm)	14.5
	Wavelength (nm)	1556.26
	Line-width(kHz)	~100

LPF	3-dB bandwidth (GHz)	1.1
EDFA	Wavelength range (nm)	1530-1560
	Noise Figure	Max. 5dB

A training sequence (TS) is added for channel estimation and symbol synchronization. These electrical base-band OFDM signals (the OFDM signals are generated offline with Matlab) uploaded into a commercial arbitrary waveform generator (AWG). The sample rate of the AWG is 2.5 GSamples/s. The peak-to-peak voltage of the signals is 2V. A continuous wave (CW) light wave is generated from an external cavity laser (ECL) at a wavelength of 1556.26nm and linewidth of 100 kHz with power output of 14.5 dBm. The output power of optical OFDM signals after MZM is -2 dBm. The optical OFDM signals are amplified by an erbium doped fiber amplifier (EDFA) with fiber launch power of 2.75 dBm and transmitted over 70 km SMF. A tunable attenuation (ATT) is used to change the power of the optical signal. At the receiver, the optical OFDM signals are converted into electrical signals after PIN photodiode (PD-83446A). The electrical OFDM signals are captured by a 10 Gsample/s Tektronix (TDS684B) real-time oscilloscope and stored for off-line processing by MATLAB program as an OFDM receiver.

The electrical signal from the real-time oscilloscope is resampled, and then is synchronized. And the signal passes through a serial-to-parallel converter and then CP is removed. After that, the waveforms are converted to OFDM subcarriers using FFT. In the frequency-domain, each channel is estimated by TS so as to compensate the distortion, then de-new spreading code. Each BPSK channel is demodulated to produce N parallel data channels, and then converted into a single data channel by using the parallel-to-serial converter. Finally, we measure the BER performance of the four types of OFDM signals.

3.3.2 Results and discussion

Figure 3.4 shows the CCDF versus PAPR of OFDM signals. It can be seen that, with the same subcarrier and at the CCDF of 10^{-4}, the PAPR of new spreading-OFDM signal (BPSK) can be improved by 1.5dB and 4.6dB compared with the CI-OFDM signal (4QAM), and the original signal (4QAM), respectively.

The experimental results show that the new spreading code makes signal more stable than CI code and original system. Thus, it can decreasingly produces nonlinear noises

from the nonlinear components than CI code and original system. Meanwhile, the PAPR of new spreading signal with 512 subcarriers is little bigger than that of new spreading signal with 256 subcarriers.
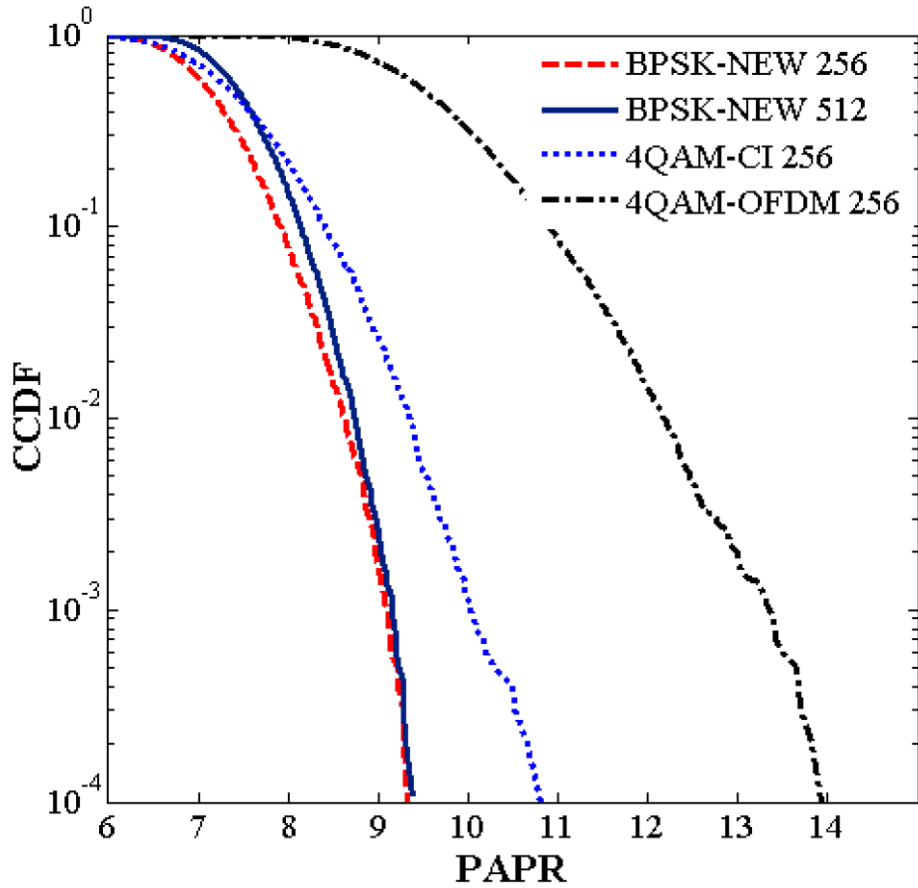
Figure 3.4: CCDF versus PAPR of OFDM signals

The net bit rate with 256 subcarriers is about 1.726 Gbit/s in the BPSK-modulated OOFDM system ($R_{BPSK-NEW256}$ = 256 x 201/((496 + 288 x 257) x 0.4) = 1.726).

The net bit rate with 256 subcarriers is about 1.718 Gbit/s in the 4QAM-modulated OOFDM system ($R_{4QAM-CI256}$ = $R_{4QAM-OFDM256}$ = 256 x 200/((496 + 288 x 257) x 0.4) =1.718).

The net bit rate with 512 subcarriers is about 1.693 Gbit/s in the BPSK-modulated OOFDM system ($R_{BPSK-NEW512}$ = 256 x 393/((496 + 576 x 257) x 0.4) = 1.693).

Figure 3.5 shows a comparison of BER performance for 4QAM CI signal, 4QAM original signal, and BPSK-new spreading signals, at a fiber launch power of 2.75 dBm and length of SMF is 70 km. At the BER of 10^{-3} and with 256 subcarriers, the received optical power is about -26, -25.4 and -23.9 dBm for the BPSK new spreading signal,

4QAM CI signal, and 4QAM original signal, respectively. The experimental results show that the BER performance based on the new spreading signal can be improved, although the $R_{BPSK-NEW256}/R_{4QAM-OFDM256}=1.005$. The received sensitivity optical power of the BPSK new spreading signal can be improved by 0.6, and 2.1dB, when compared with the case of using 4QAM CI signal, and 4QAM original signal, respectively.
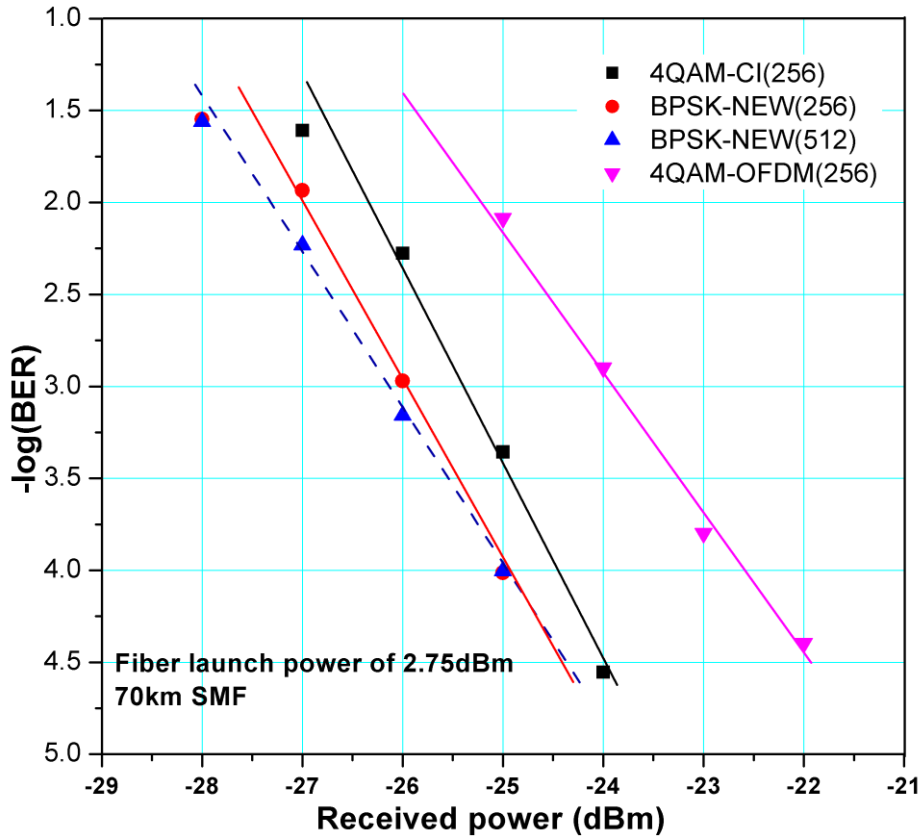
Figure 3.5: BER curves of OFDM signals

The experimental results also show that, at the BER of 10^{-3}, the received optical power is about -26.2, and -26 dBm for the BPSK new spreading signal with subcarrier of 512 and 256, respectively.

This result proves that new spreading code with low cross correlation and has better orthogonality property proportional to the high number of subcarrier.

3.4 Conclusions

In this chapter, we proposed a new spreading code to reduce the high PAPR in IM/DD optical OFDM systems. The effect of new spreading code in the BER performance of the system was experimentally demonstrated. At a CCDF of 10^{-4}, the PAPR of new spreading signal was reduced by 1.5 and 4.6 dB, compared with the 4QAM CI signal

and 4QAM original signal, respectively, when number of subcarriers was 256. The experimental results showed that, the receiver's sensitivity of optical OFDM signal with the new spreading code was better than that of original signals. Meanwhile, the net bit rate of signal with new spreading code was bigger than that of original signal. At the BER of 10^{-3}, the received power of optical OFDM signal with new spreading code was more sensitive than the 4QAM CI signal, and 4QAM original signal by 0.6 and 2.1 dB, respectively. The result also proves that new spreading code with low cross correlation has better orthogonality property proportional to the high number of subcarrier. By using new spreading code in IM/DD-OOFDM system, it can not only reduce PAPR, but it is also capable of supporting 2N+1 users, thus to obtain better BER performance.

Although new spreading code can improve BER performance and enhance the channel capacity, but BER performance still is limited. Various PAPR reduction methods have been developed with trade-off between PAPR reduction capability and loss in data rate, degradation of BER performance, increase in signal power and augmentation in computational complexity. That's why a specific PAPR reduction scheme can't be considered as a best solution. To get more efficient performances of system, the good approach may be the combination of different schemes. Recently, some hybrid techniques tended to be the combination of techniques such as PTS-clipping [81], Hadamard - companding transform technique [82], clipping and filtering based on DCT/IDCT [83], Hadamard - clipping and filtering based on DCT/IDC [84], etc...

Therefore, next chapter a novel new hybrid peak-to-average power ratio reduction technique based on carrier interferometry codes and companding technique for optical direct detection orthogonal frequency division multiplexing system is proposed and presented in detail.

Chapter 4: **NEW HYBRID METHOD FOR PAPR REDUCTION BASED ON CARRIER INTERFEROMETRY CODES AND COMPANDING TECHNIQUE**

4.1 Introduction

Following the discussion on the PAPR reduction technique in chapter 3 which proposed a novel new hybrid method PAPR reduction technique based on carrier interferometry codes and companding technique for optical direct detection orthogonal frequency division multiplexing system[85], this chapter still focus in the same way.

In case of large transmission distance between two link of the IM/DD Optical OFDM, the launch power must be high, it result in excessive nonlinear noise [40], and the reducing high PAPR is necessary.

This chapter proposes a novel hybrid method to reduce the fiber nonlinearity through reducing the high PAPR in IM/DD optical OFDM systems. This method based on joint companding technique and CI codes. In here, we use a nonlinear companding scheme, which means that there is only companding at the transmitter and no expanding at the receiver. The companding at the transmitter is carried out by using of μ-law and linear algorithm to keep the output power the same as the origin.

Our experimental results show that this hybrid method is able to offer better performance in terms of both PAPR reduction and BER for OFDM systems.

The remainder of the chapter is organized as follows. While section 4.2 describes the principle of hybrid method, section 4.3 introduces the experimental setup and results. Finally, conclusive remarks are discussed in section 4.4.

4.2 Principle of hybrid method

In this section, the CI codes, and the companding techniques for PAPR reduction of OFDM signal is reviewed. After that the structure of hybrid method in the IM/DD optical OFDM transmission system is presented.

4.2.1 OFDM with CI spreading

Figure 4.1(a) describes the OFDM transmitter with CI codes. In CI-OFDM system, each parallel data symbol is modulated onto all of the *N* carriers, and a reparability of each parallel data symbol is maintained by using carefully selected phase offsets.
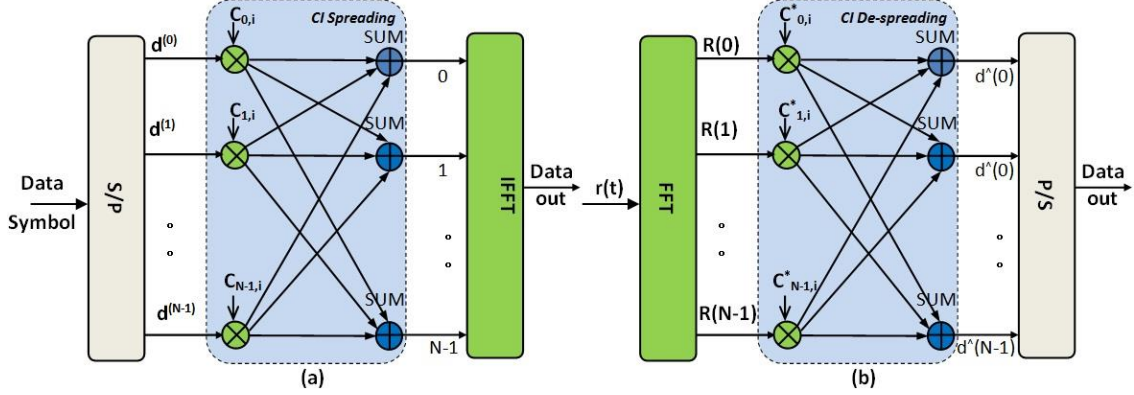
Figure 4.1: Structure of OFDM with CI codes

The CI-OFDM at Ref. [43] only BPSK modulation is considered. In this paper, we extend CI/OFDM architecture to study its operation with 4QAM constellations as suggested by Wu et al [86], and Ali et al [87]. The signal with CI codes (contain *N* different codes) is expressed as following

$$S(t) = \frac{1}{\sqrt{N}} \sum_{k=0}^{N-1} \sum_{i=0}^{N-1} d^{(k)} e^{j(2\pi i \Delta f t)} C_{(k,i)}$$

(4.1)

where *d* is the data symbol, Δf is the carrier spacing of IFFT, and *N* is the number of subcarriers.

C(k,i) are coefficients of CI codes. *C(k,n)* structures for *N* subcarriers are

$$C_{(k,n)} = e^{j\left(\frac{2\pi}{N}\right)kn},$$
$$for\ n = 0,1,..,N-1; k = 0,1,..N-1$$

(4.2)

The PAPR of the CI-OFDM signal can be defined as

$$PAPR = \frac{\max |S(t)|^2}{E\{|S(t)|^2\}}$$

(4.3)

where $E\{\bullet\}$ denotes the expectation operation. $E\{|S(t)|^2\}$ is equal to the variance σ^2, since the symbols are zero mean. The statistics for the PAPR of an OFDM signal can be given in terms of its complementary cumulative distribution function (CCDF).The

CCDF of PAPR is defined as the probability that the PAPR of the OFDM symbols exceeds a given threshold PAPR0. The CCDF for an OFDM signal is expressed as

$$CCDF = P(PAPR > PAPR0) \tag{4.4}$$

Figure 4.1(b) describes the OFDM receiver with CI codes, the received signal $r(t)$ from the channel is converted into to frequency domain using FFT. The obtained signal is de-spread with complex conjugate codes $C^{*}_{(k,n)}$, and combined. Finally, the hard decision device is employed to create a final decision of $\hat{d}(k)$.
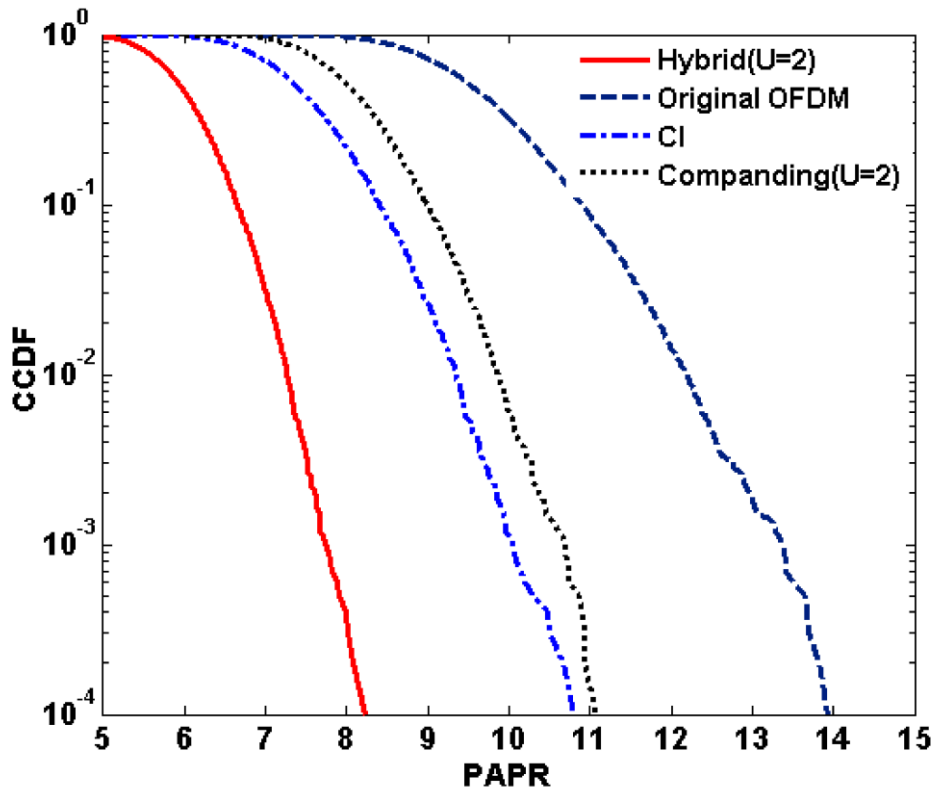
Figure 4.2: CCDF versus PAPR of OFDM signals, when μ =2 for different techniques

Figure 4.2 shows the CCDF versus PAPR of OFDM signals. It's noticeable that the PAPR of the OFDM signal with the CI codes is reduced by 3.1 dB compared with that of the original OFDM when the CCDF is 10^{-4}.

4.2.2 Companding technique

In this section, we review the companding technique for PAPR reduction of OFDM signal. The traditional μ-law companding algorithm was first proposed by Wang et al [55, 58] in speech processing. In traditional companding technique [58], OFDM signals are companded at the transmitter and expanded at the receiver. The amplitudes of the small signals are enlarged while those of the large signals remain the same. As the average

power is enhanced through enlarging the small signals, so we use a linear companding to the OFDM signals for the sake of keeping the signals of equal average power as Ref. [55]. The signal S_{out} at the end of transmitter using μ-law companding [58] can be expressed as

$$S_{out} = \frac{A \cdot sgn(S_{in}) \ln(1 + \mu \,|\, S_{in} / A \,|)}{\ln(1 + \mu)} \qquad (4.5)$$

where S_{in} is the output signal after N-point IFFT, here is the signal of CI codes, μ is the companding coefficient, and A is the peak amplitude of the signal S_{in}.

According to Wang et al [55], when N sufficiently large, with Taylor's series, $S_{out} \approx S_{in} \cdot \mu \,/ \ln (\mu + 1)$. The average power of the companded signal is amplified by the coefficient $K = \mu \,/ \ln (\mu + 1)$. Hence, we use a linear companding by multiplying a constant coefficient $K' = 1/K$ to keep the signal power unchanged. The signal at the end of the transmitter is then evolved to

$$S'_{out} = \frac{A \cdot sgn(S_{in}) \ln(1 + \mu \,|\, S_{in} / A \,|)}{\mu} \qquad (4.6)$$

From Eq. (4.6), when μ increases, the reduction rate of the peak power is decreasing. But, if μ is big, BER performance will be reduced, so μ must be chosen a small value [82, 88, 89]. In this paper, we choose the μ is 2 such as Ref. [82, 88, 89].

According to Hou et al [76], the system without expanding at the receiver has a better BER performance. So in this paper, we take the nonlinear companding scheme, which has μ-law companding at the transmitter but lacks de-companding at the receiver.

It can be seen from Figure 4.2 that the PAPR of nonlinear companding scheme can be improved by 2.8 dB compared with the original OFDM system at the CCDF of 10^{-4}, when μ is 2.

4.2.3 The structure of hybrid method

The hybrid PAPR reduction method, proposed in this paper, used CI codes and a nonlinear companding scheme. The first PAPR reduction method, which is accomplished by transmission of each bit over each of the N carriers through the novel use of CI phase codes, and the second PAPR reduction method perform a variable attenuation of the signal which depends on its amplitude.

Figure 4.3 shows the principle of our proposed an IM-DD optical OFDM transmission system with hybrid method.
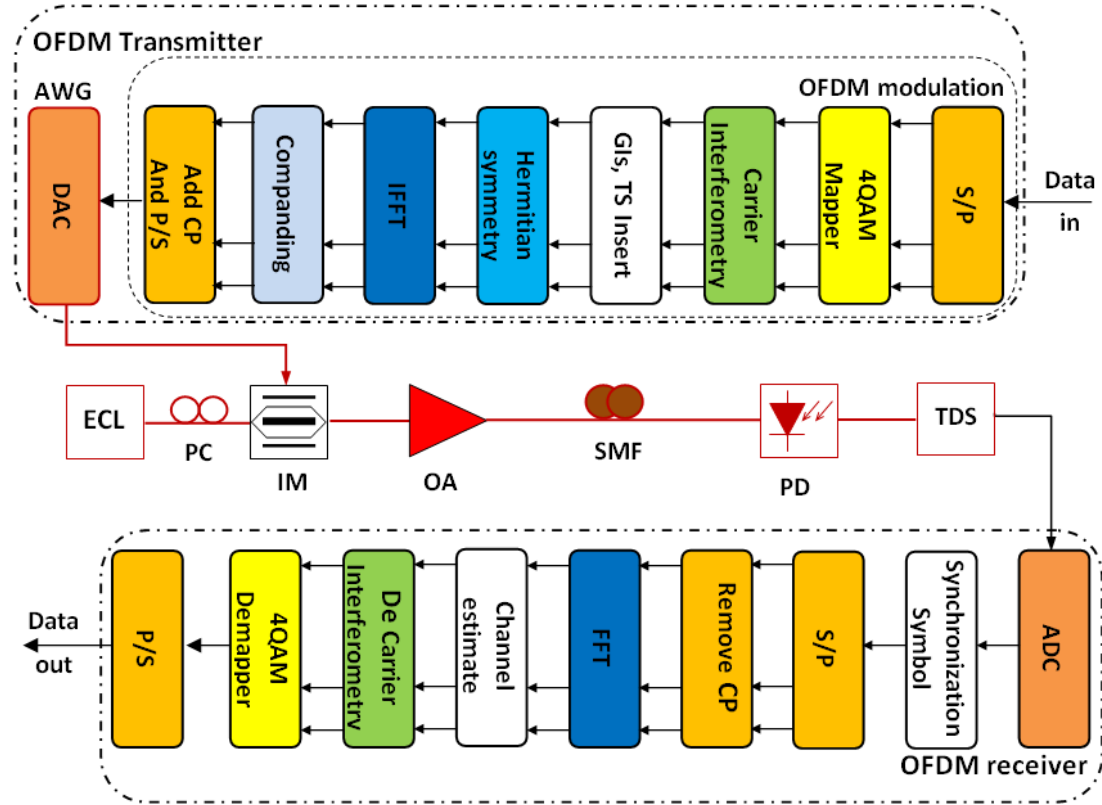
Figure 4.3: Principle of the intensity-modulation direct-detection (IM/DD) optical OFDM transmission system with hybrid method. LD: laser diode, PC: polarization controller, IM: intensity modulation, OA: optical amplifier, PD: photodiode.

At the transmitter side, the pseudorandom binary sequence (PRBS) data are converted into parallel data by S/P converter. The parallel data is mapped onto a 4QAM format then spread by CI phase codes (detailed in Section 4.2.1), and the data passed through an *N* IFFT block. The IFFT produces a complex-valued time domain waveform containing a superposition of all of the subcarriers. After IFFT, the OFDM symbols pass through a nonlinear companding scheme (detailed in Section 4.2.2), and then the prefix is added. A digital- to-analog converter (DAC) is used to generate the electrical baseband OFDM signal. The training sequence (TS) is used for channel estimation and symbol synchronization. The cyclic prefix (CP) is used to mitigate the ISI. Next, the electrical baseband OFDM signal converted by a DAC is used to drive an IM to modulate the optical carrier of laser diode (LD). The generated optical OFDM signal is boosted by an optical amplifier (OA) and transmitted over single mode fiber (SMF).

At the receiver side, the electrical signal from the photodiode is sent into an ADC to produce a digital signal, and then the signal passes through a serial-to-parallel converter and the waveforms are converted to OFDM subcarriers using FFT. Once in the

frequency-domain, each channel is estimated by TS to compensate for distortion due to the optical and electrical paths, then de-spread CI codes. After that, each 4QAM channel is demodulated to produce N parallel data channels, and these can be converted into a single data channel by parallel-to-serial converter.

In this chapter, usually the channel estimation and the synchronization symbol are realized by using training sequence (TS). Synchronization symbol is used for finding the correct symbol start, and auto-correlation algorithm or cross-correlation algorithm can be used for this purpose. However, findings from Fort et al [90], indicate that the cross correlation algorithm can provide better performance at a low signal-to-noise ratio due to the averaging process of the correlator. Here, the cross-correlation property of TS is used to calculate the timing metric function instead of the auto-correlation property. The cross correlation is expressed as:

$$P(d) = \sum_{k=0}^{N_t-1} t(k).r(k+d), \tag{4.7}$$

where $t(k)$ is the transmitted TS of length $N_t = N + N_{CP}$, N_{CP} is length of the cyclic prefix, and $r(k)$ is the received signal. The TS is generated by modulating the odd subcarriers (excluding the subcarriers at high frequencies) with binary phase shift keying (BPSK) symbols, while the even subcarriers and the subcarriers at high frequencies are filled with zeros. TS is produced by transmitting BPSK symbols on the odd subcarriers, it can reduce the signal-to-signal beating interference (SSBI) in the direct-detection optical OFDM receiver [91]. After the optical OFDM signal is detected by a photodiode, the BPSK symbols on the odd subcarriers will not be interfered by SSBI. Therefore the TS can also be used to estimate the channel responses of all channels without SSBI via interpolation.

In the optical fiber, in a short period of time the channel response can be considered approximately as a constant and the difference of channel frequency responses over every two adjacent subcarriers is small. Thus, the channel information on the even subcarriers can be estimated from the two adjacent odd subcarriers through frequency-domain interpolation. According to Chen et al [80], the even channel response can be obtained by linear interpolation. It can be expressed as

$$H_{even}(i) = \frac{H_{odd}(i-1) + H_{odd}(i+1)}{2}, \tag{4.8}$$

where $H_{even}(i)$ denotes the channel response on the ith subcarrier with even index, $H_{odd}(i-1)$ and $H_{odd}(i+1)$ are the channel response for two adjacent odd subcarriers.

Figure 4.2, indicates that the hybrid technique reduce peak power compared with all the others. For example, at the CCDF of 10^{-4} and $\mu=2$, the PAPR of OFDM signal with hybrid technique can be reduced by 2.6, 2.9 and 5.7 dB when compared with the OFDM signals only with CI codes, nonlinear companding scheme and original OFDM, respectively. By comparing the case of using only the CI codes or only a nonlinear companding technique, the hybrid method can provide better system performance in terms of PAPR reduction.

4.3 Experimental setup and results

4.3.1 Experimental setup

Figure 4.4 describes the experimental setup of the IM/DD optical OFDM transmission system. Three types of signal are used in our experimental configuration such as the OFDM signals without any technique, with CI codes, with companding technique only and with the proposed hybrid method. The parameters of the experiment setup are shown in the Table 1.

The OFDM signal is generated offline with Matlab and uploaded into a commercial arbitrary waveform generator (AWG) (OFDM signals with the pseudorandom pattern length of 51200). The sample rate of the AWG is 2.5 GSamples/s. The peak-to-peak voltage of the signals is 2V. A continuous wave (CW) light wave is generated from an external cavity laser (ECL) at a wavelength of 1556.26 nm and line-width of 100 kHz with power output of 14.5 dBm. The output power of optical OFDM signals after MZM is about 3dBm. The optical OFDM signals are amplified by an EDFA with different launch power and transmitted over 100 km SMF. The optical OFDM signals are converted into electrical wave signals via PIN photodiode (PD-83446A), then sampled and recorded by TDS (TDS-6804B). In the receiver, we use the Matlab program to process the waveform recorded by TDS. We measured the PAPR and BER performance of the received signals.

Table 4.1: The parameters of experiment

Items	Sub items	Value
OFDM	FFT	256
	Subcarriers for data	200
	CP	32
	GI	56
	PRBS length	51200
	Modulation	4QAM
	OFDM symbol	256
Training sequence	Training sequence	1
ECL	Power output (dBm)	14.5
	Wavelength (nm)	1556.26
	Line-width (kHz)	100
MZM	Half-wave voltage (V)	4
	Bias voltage (V)	2.1
	Power output (dBm)	3
Fiber	Fiber length (km)	100
	Attenuation (dB/km)	0.19
	Dispersion (ps/nm/km)	16.75
	Dispersion slope (ps/nm^2/km)	0.075
	Effective area (um^2)	80
	n_2 (m^2/w)	2.6e-20
	SNR (dB)	15
AWG(AWG710)	Sample rate (GSa/s)	2.5
	Vpp (V)	2
PD(83446A)	Wavelength range (nm)	1200 to 1600
	Auxiliary out bandwidth (MHz)	0.1 to 1500
LPF	3-dB bandwidth (GHz)	1.1
EDFA	Wave length range (nm)	1530-1560
	Noise Figure	Max. 5dB
TDS	Sample rate (GSa/s)	10
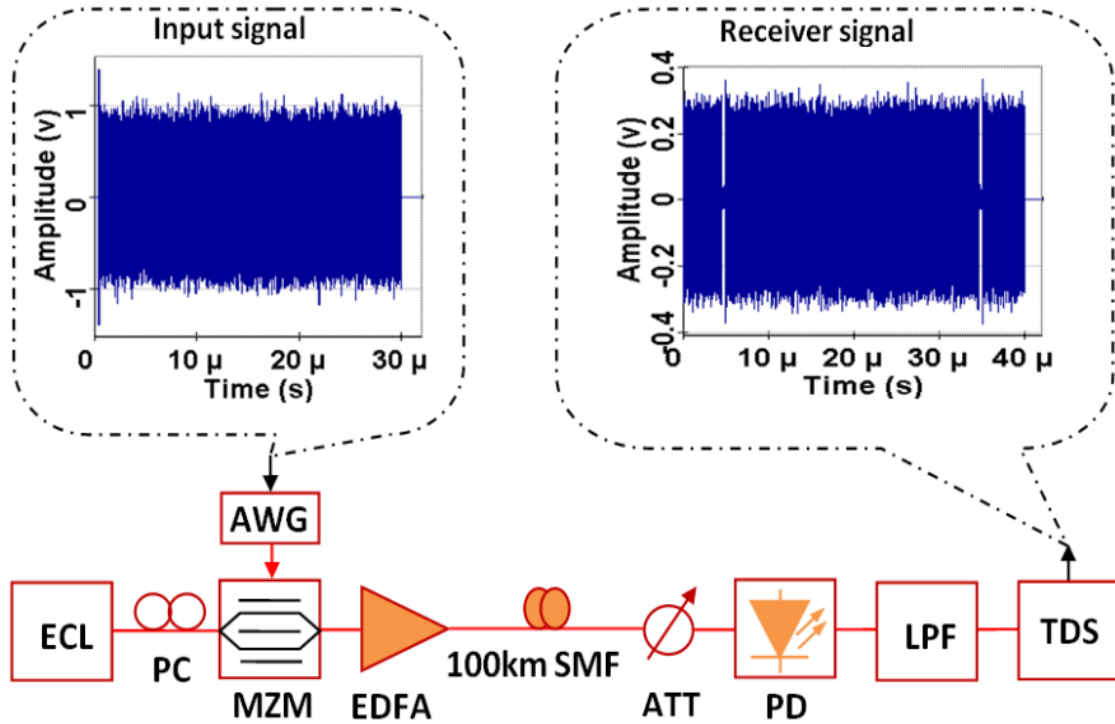
Figure 4.4: The implementation for the IM-DD OFDM transmission system with the hybrid method. ATT: attenuator, ECL: external cavity laser, PC: polarization controller, MZM: Mach–Zehnder modulator, EDFA: Erbium doped fiber amplifier, PD: photodiode, TDS: real-time/digital storage oscilloscope, and LPF: low pass filter

4.3.2 Results and discussions

The net bit rate of 4QAM OFDM signal is about 1.718 Gbit/s (R_{4QAM}=256 x 200/((496 + 288 x 257) x 0.4) =1.718).

Figure 4.5 shows a comparison of BER performance for original OFDM signal, companding signal, CI signal and hybrid signal, when μ =2, at a fiber launch power is 3dBm and length of SMF is 100 km. At the BER of 10^{-4}, the received optical power of the hybrid signal, CI signal, companding signal and original OFDM signal is about -25.8, -24.2, -24, and -22.1 dBm, respectively. The results show that the BER performance of OFDM signal with hybrid method (μ=2) is the best. The received sensitivity optical power of the proposed hybrid method can be improved by 1.6, 1.8, and 3.7 dBm when compared with the case of using only CI codes, companding technique, and original OFDM, respectively.
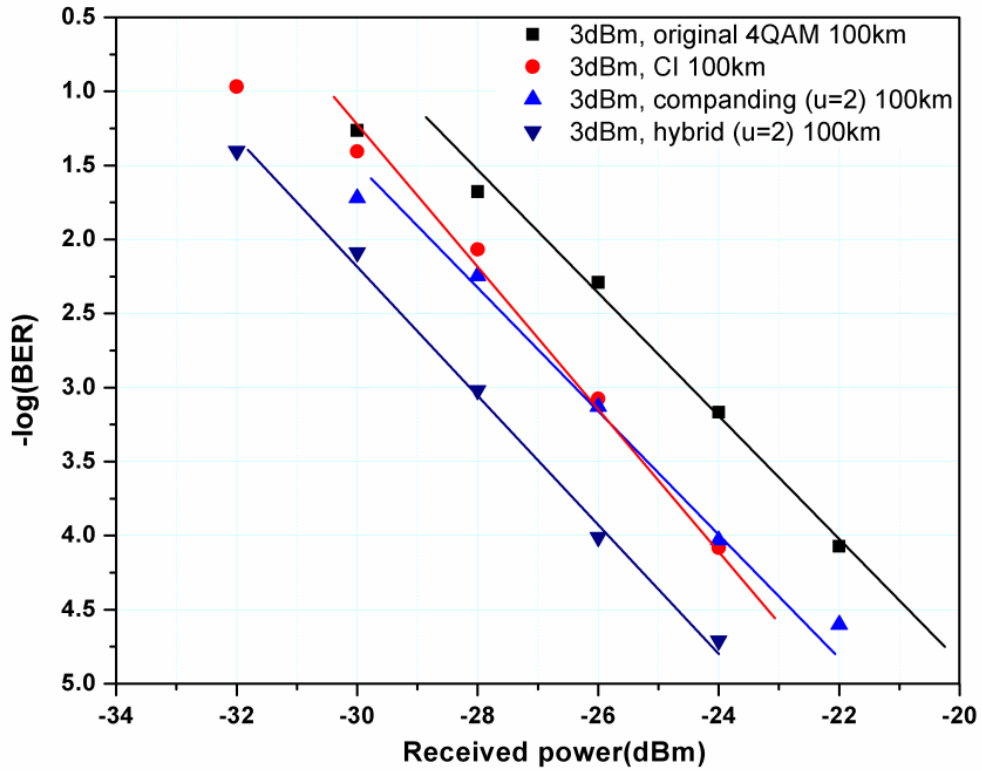
Figure 4.5: BER curves of OFDM signals at 3 dBm launch power after transmission over 100km SMF, when μ =2

Figure 4.6: BER curves of OFDM signals at 6 dBm launch power after transmission over 100 km SMF, when μ =2

In the same way of the Figure 4.5, the Figure 4.6 and Figure 4.7 also compared the BER performance of original OFDM signal, companding signal, CI signal and hybrid signal, when $\mu = 2$ with 6 dBm and 9 dBm of fiber launch power and after transmission over 100 km SMF. At BER of 10^{-4}; when the fiber launch power is 6 dBm, the received optical power is about -26.6 dBm for signal with hybrid method, -24.9 dBm for CI codes, -24.6 dBm for companding technique and -22.4 dBm for original OFDM; in case of fiber launch power of 9 dBm, the received optical power is about -27.6 dBm for signal with hybrid method, -25.7 dBm for CI codes, -25.2 dBm for companding technique and -22.6 dBm for original OFDM.

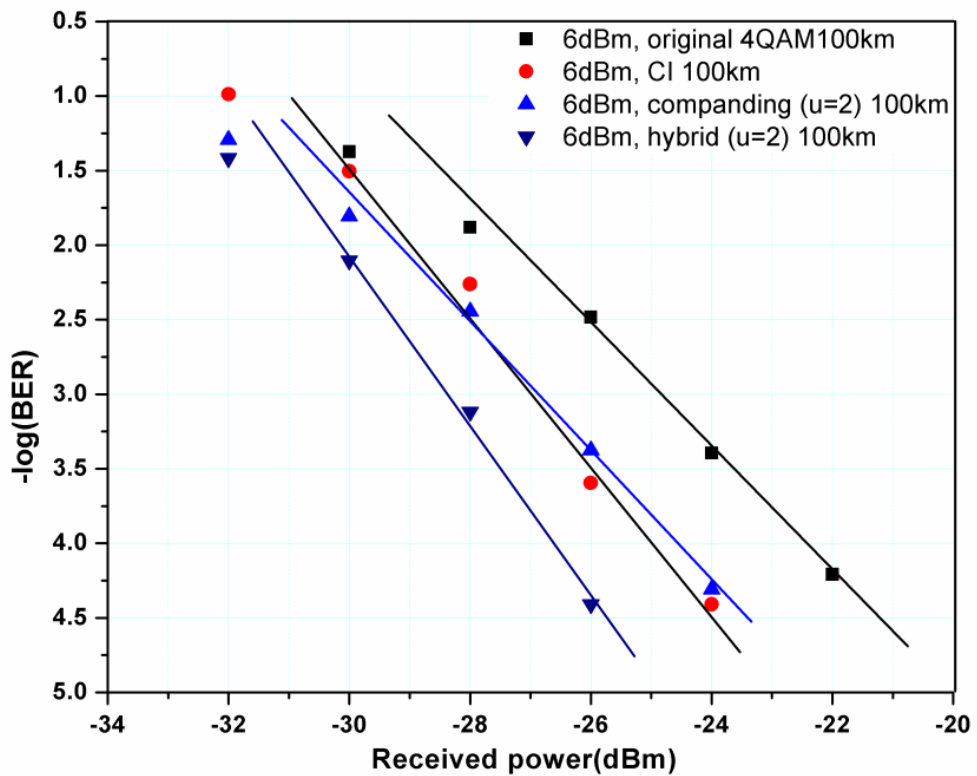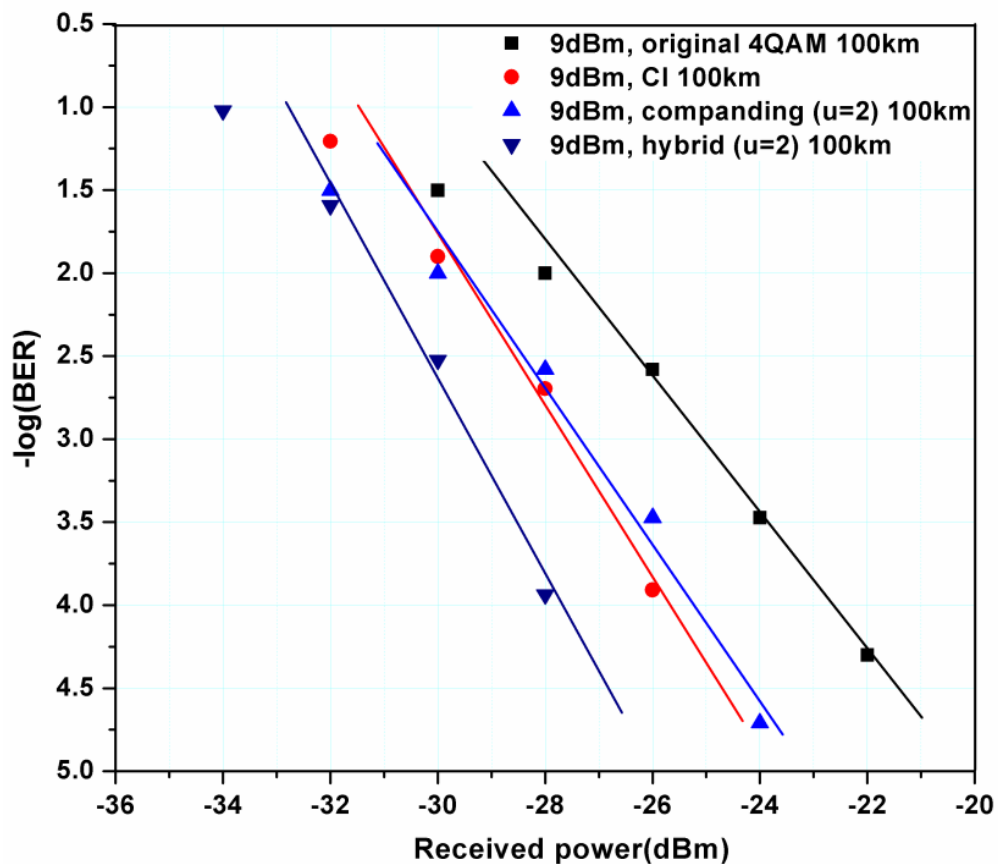Figure 4.7: BER curves of OFDM signals at 6 dBm launch power after transmission over 100 km SMF, when μ =2

The results of Figure 4.5, Figure 4.6, and Figure 4.7 show that, when the optical fiber launch power increases, the receiver sensitivity of optical OFDM signals also increase. But the receiver sensitivity of the optical OFDM signal with the hybrid method is better than the others signals.

Figure 4.8 shows BER via launch power of optical OFDM signals at received power of -26 dBm after transmission over 100 km SMF. At the same launch power, BER performance of hybrid method is the best, BER performance of original is the worst. When the launch power increases, the BER of hybrid method is faster decreasing than other techniques. From the Fig. 4.8, it can be seen that the hybrid method is better than that of other methods. The BER of 9dBm to fiber is lower than that of 3dBm to fiber, it means that there is no effect of the nonlinear.
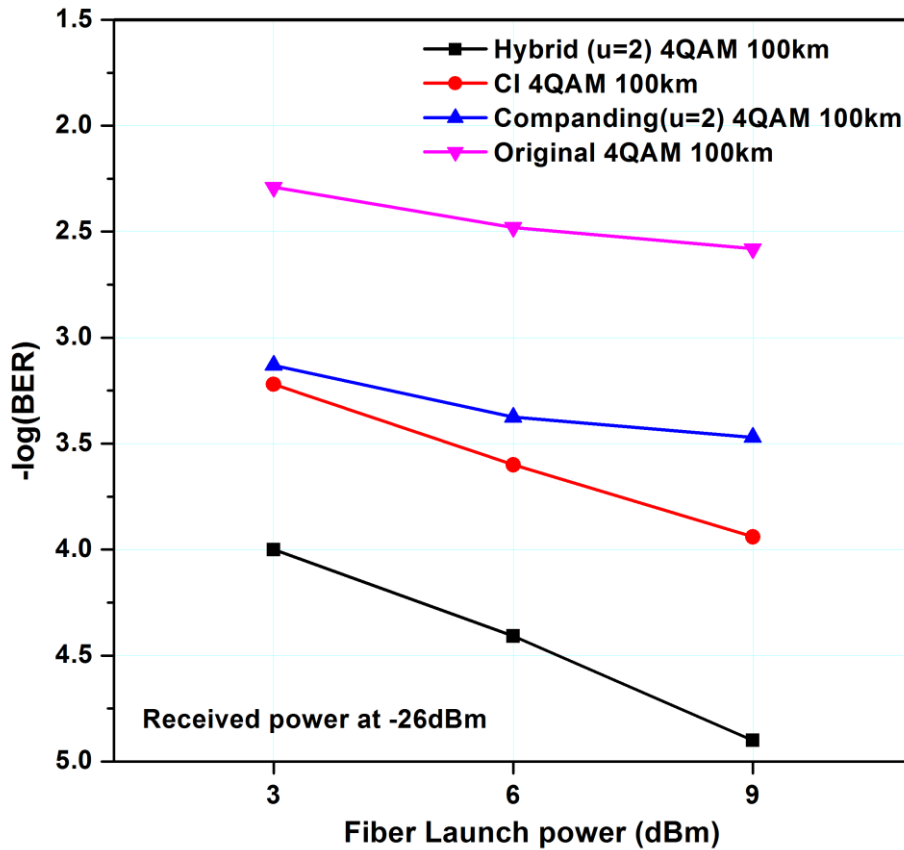
Figure 4.8: BER via launch power of OFDM signals after transmission over 100 km SMF, when μ =2.

4.4 Conclusion

In this chapter, we proposed and experimentally demonstrated a new hybrid method to reduce the PAPR of signal in IM/DD optical OFDM systems. The effect of our proposed hybrid in the BER performance of the system has been experimentally demonstrated. At a CCDF of 10^{-4}, the PAPR of OFDM signal with the hybrid method is reduced by 5.7 dB, while with the CI codes and the companding technique are reduced by 3.1 and by 2.8 dB, respectively comparing with the original OFDM. The

experimental results show that, at the same fiber launch power, the receiver sensitivity of optical OFDM signal with the hybrid method is better than signal with CI codes, with companding technique and with the original OFDM. At the BER of 10^{-4}, the received power of optical OFDM signal with hybrid method is more sensitive than the original OFDM by 3.7, 4.2, and 5 dB in case of 3, 6, and 9 dBm fiber launch power, respectively. It can be clearly seen that the proposed system can improve the received sensitivity when the optical launch power is increasing. The reason is that the hybrid method could reduce the PAPR much more effectively than the other two techniques and thus suppresses the nonlinear transmission impairments to the highest degree.

Compared to PAPR reduction scheme based on new spreading code in chapter 3, the hybrid method can significantly reduce the PAPR and can get better BER performance than new spreading code method. At the CCDF of 10^{-4}, the PAPR of OFDM signal with the hybrid method is reduced by 5.7 dB, while with the new spreading code method is reduced by 4.6 dB comparing with the original OFDM. The experimental results also indicated that, at the smaller BER limit FEC, the receiver sensitivity of the optical OFDM signal of the hybrid method is better than of new spreading code when compared to origin signal. Meanwhile the computational complexity at receiver of hybrid method is less than of new spreading code. Because the hybrid is multiplied with a matrix $C^*[N,N]$, while the new spreading code is multiplied with a matrix $C^*[2N+1,N]$.

This chapter presented a novel hybrid method to reduce the fiber nonlinearity through reducing the high PAPR in IM/DD optical OFDM systems. This hybrid was able to offer better performance in term of both PAPR reduction and BER for OFDM systems. However, because of using CI codes at the transmitter, so at the receiver had to be de-CI codes. Therefore, the hardware at the receiver is more complex than that of the original system. To overcome this problem, a novel new binary particle swarm based on dummy sequence insertion for PAPR reduction in IM/DD OOFDM system without side information will be presented in next chapter.

Chapter 5: **NEW BINARY PARTICLE SWARM OPTIMIZATION ON DUMMY SEQUENCE INSERTION METHOD FOR PAPR REDUCTION**

5.1 Introduction

A novel new binary particle swarm optimization (NBPSO) [92] method based on dummy sequence insertion (DSI) [45] in this chapter is proposed and experimentally demonstrated for PAPR reduction in the IM-DD OOFDM system. The methods for PAPR reduction have been used in chapter 3, 4 and its references almost have to use side information or cause signal distortion, which make the system more complex or produce significantly clipping noise, out of band radiation.

The DSI [45, 93] method insert dummy sequence into the transmission data block for PAPR reduction before the IFFT stage. In the DSI method [45], a complementary sequence and the combination of the correlation sequence are considered as dummy sequence, which will be discarded at the receiver, thus, the side information is not necessary. Moreover, compared with the conventional PTS or SLM method, the BER performance of the method is better in the case of the errors in the side information about the phase rotation. However, in some case the computation is high. In order to solve complex computational problems, various heuristic approaches have been adopted by researches including Genetic algorithm, Tabu search and PSO. PSO [94, 95] is one of optimization techniques, which can generate high quality solution within shorter calculation on some optimization problems. The origin version of the PSO [94] operates in continuous space and the binary PSO (BPSO) [95] operates on discrete binary variables. The PSO technique has been using in many fields such as power systems [67, 96, 97], neural network learning [98, 99], data cluster [100], FPGA routing [101], multi-user OFDM [102], and for PAPR reduction in wireless OFDM system [93, 103, 104]. During utilization and research PSO and BPSO, some researchers are shown that standard PSO and BPSO cannot converge well. To overcome this problem with BPSO, a novel NBPSO is proposed. So in this chapter we use propose a novel NBPSO based on DSI method to reduce the nonlinearity of equipment in IM/DD OOFDM system.

This chapter is organized as follows: Section 5.2 describes the principle of DSI and NBPSO. Then, we introduce the experimental setup and results in Section 5.3. Finally, the concluding remarks are given in Section 5.4.

5.2 System Model

5.2.1 Dummy sequence insertion method

The DSI method [45] can reduce the PAPR by inserting a dummy sequence in the subcarriers of the OFDM system. Dummy sequence is used for only PAPR reduction without any channel information. At the receiver, dummy sequence can be discarded after FFT stage. It is different from the conventional PTS and SLM methods. Therefore, the DSI method can greatly reduce the complexity of the receiver. And it is independent of the dummy sequence error. Figure 5.1 illustrates the structure of the DSI data. In this paper, DSI with method 3 of Ref. [93] is used, and 16QAM format is considered. Here, the total number of subcarriers in the OFDM signal is M, and the number of subcarriers reserved for the dummy sequence is L; therefore, there are N = M – L subcarriers available for data transmission. And the number of dummy sequence bit is K=4xL
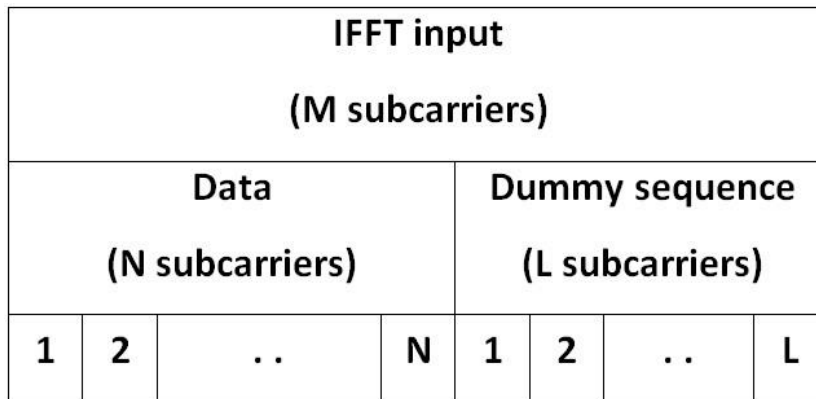
Figure 5.1: DSI data block using the complementary sequence.

From Figure 5.1, the output signal of the IFFT can be expressed as follows:

$$y(t) = \text{IFFT}([x\ s]^t) \tag{5.1}$$

where $y=[y_1, y_2, .., y_M]^t$, $x=[x_1, x_2, .., x_N]^t$ is the transmission data sequence and $s=[s_1, s_2, .., s_L]^t$ is the inserted dummy sequence. IFFT(z) implies the inverse fast Fourier transform of z, and $[\bullet]^t$ is a transpose operation.

The PAPR of the OFDM signal with DSI can be defined as

$$PAPR = \frac{\max |y(t)|^2}{E\{|y(t)|^2\}} \tag{5.2}$$

Where $E\{\bullet\}$ denotes the expectation operation. $E\{|y(t)|^2\}$ is equal to the variance σ^2, since the symbols are zero mean. The statistics for the PAPR of an OFDM signal can be given in terms of its complementary cumulative distribution function (CCDF). The CCDF of PAPR is defined as the probability that the PAPR of the OFDM symbols exceeds a given threshold PAPR0. The CCDF for an OFDM signal is expressed as

$$CCDF = P(PAPR > PAPR0) \tag{5.3}$$

Eq.(5) can be rewritten in vector form and expressed in decibels as

$$PAPR = 10\log_{10} \frac{\max |y(t)|^2}{\text{mean}\{|y(t)|^2\}} \tag{5.4}$$

5.2.2 NBPSO scheme based on DSI method

Similar to evolutionary algorithms, the PSO technique conducts searches using a population of particles, corresponding to individuals. Each single solution is a particle in the search space. A swarm of these particles moves through the search space to find an optimal position. The position and velocity are two parameters to characterize each particle.

In a L-dimensional optimization, the position and velocity of the jth particle can be represented as $z_j = \{z_{j,1}, z_{j,2}, . ., z_{j,L}\}$ and $v_j = \{v_{j,1}, v_{j,2}, . ., v_{j,L}\}$, respectively. PSO algorithm is initialized with a group of random particles and then searches for optimal by updating generations. In each iteration, particle updates itself through tracking two best positions. The first one is the local best position (p_best_j), which represents the position vector of the best solution of this particle has achieved so far. The other one is the global best position (g_best), which represents the best position obtained so far by any particle. After finding the two best values, the update of velocity and position for each particle are described as Eq. (5.6) and Eq. (5.7), respectively.

$$v_{jk}(t+1) = w.v_{jk}(t) + c_1.rand()(p\_best_{jk} - z_{jk}) + c_2.Rand()(g\_best_k - z_{jk}) \tag{5.6}$$

$$z_{jk}(t+1) = z_{jk}(t) + v_{jk}(t) \tag{5.7}$$

In the version of BPSO, the search space is considered as a hypercube in which a particle may be seen to move to nearer and farther corners of the hypercube by flipping various numbers of bits. The moving velocity is defined in terms of changes of

probabilities of that a bit will be in one state or the other. Thus a particle moves in a state space restricted to 0 and 1 on each dimension.

The key point in DSI method is to search out the dummy sequence that minimizes the PAPR of an OFDM signal. Form Eq. (5.4), the problem of PAPR reduction using DSI method can be modeled as a constrained optimization problem. It is given by

$$\text{minimize PAPR subject to s, } P_L \qquad (5.8)$$

where P_L is the total power limitation of inserted dummy sequence.

The NBPSO scheme is adopted to solve this constrained optimization problem, which can search out the global optimal dummy sequence to minimize the PAPR of an optical OFDM signal. The fitness function in this case is the Eq. (5.4), and it can be expressed as

$$f(s) = 10\log_{10}\frac{\max|y(t)|^2}{\text{mean}\left\{|y(t)|^2\right\}} \qquad (5.9)$$

The NBPSO scheme based on DSI method is illustrated in Figure 5.2, it will be described in detail as follows:
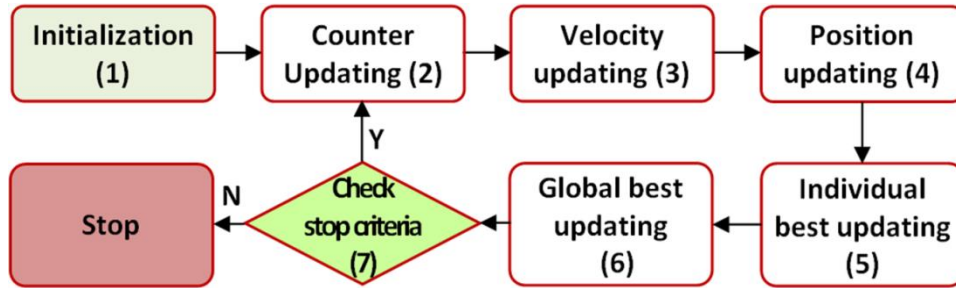
Figure 5.2: The NBPSO scheme based on DSI method.

Step 1. *Initialization* state

Firstly, the iteration counter t is reset, i.e. t=0, and P particles is randomly generated as [$Z_j(0)$, j=1, 2, .., P], where $Z_j(0)$=[$z_{j,1}(0)$, $z_{j,1}(0)$, . ., $z_{j,K}(0)$]^t, and $z_{j,k}(0)$ denotes the kth bit of jth particle at t=0. A vector of K bits represents the position of a particle, and signifies a probably desired dummy sequence. Then, the initial velocities of all particles are set to zero, such as, [$V_j(0)$, j=1, 2, .., P]=0, where $V_j(0)$=[$v_{j,1}(0)$, $v_{j,2}(0)$, . ., $v_{j,K}(0)$]^t.

Secondly, modulate and evaluate the fitness function of each particle in the initial population based on the Eq. (5.9), and we set p_best$_j$=$Z_j(0)$ and F_{fnj}=$F_j(0)$, j=1, 2, .., P,

where p_best$_j$=(p_best$_{j1}$, p_best$_{j2}$, .., p_best$_{jK}$) and $F_{\text{fn}j}$ register the individual best position for the jth particle and its fitness value of the jth particle at t=0.

Thirdly, we find the best fitness value $F_{\text{bestfn}} = \min([F_{\text{fn}j}, j=1, 2, .., P])$ registering the fitness values of all initial particles, and set the particle of F_{bestfn} as the global best g_best, which has an fitness value F_{bestfn}.

Finally, set the initial values of the inertia weigh w and constants c_1 and c_2, which used in velocity updating.

Step 2. *Iteration counter updating* state

Update the generation counter as t=t+1.

Step 3. *Velocity updating* state

In the NBPSO scheme, each v_{jk} represents the probability of bit z_{jk} taking the value 1, and v_{jk} must be constrained to the interval [0.0, 1.0]. By defining a function $S(v_{jk})$ of the kth element in the jth particle, it is updated according to the following equation:

$$S(v_{jk})=2\text{x}|(\text{sigmoid}(v_{jk})\text{-}0.5)| \tag{5.10}$$

with

$$Sigmoid(v_{jk}) = \frac{1}{1+e^{-v_{jk}}}$$

where c_1 and c_2 are positive constants, rand() is a quasi-random number selected from a uniform distribution in [0.1, 1.0], w is the inertia weight, and v_{jk} is limited in the range of [- v_{max}, $v_{\max}$].

Step 4. *Position updating* state

Based on the updated velocities, the position of each particle will be changed by the following equation:

$$If\ \ rand()< S(v_{jk}(t+1))\ then\ z_{jk}(t+1)=exchange(z_{jk}(t))\ else\ \ z_{jk}(t+1)=z_{jk}(t) \tag{5.11}$$

Step 5. *Individual best updating* state

Each particle is evaluated by fitness function on the renewed position. If there is $F_j(t)<F_{\text{fn}j}$, $j=1, 2,..., P$, update individual best as P_best$_j$=Z$_j$(t) and $F_{\text{fn}j}$=$F_j(t)$, and go to the global best updating state.

Step 6. *Global best updating* state

Searching for the minimum fitness value $F_{\min}$ from F_{fnj}, $j=1, 2, ..P$, where min is the index of particle with minimum fitness, i.e., min $\in \{1, 2, .., P\}$. If $F_{\min} < F_{bestfn}$, then the global best is updated as $g\_best = Z_{\min}(t)$, and $F_{bestfn} = F_{\min}$.

Step 7. *Stop criteria checking* state

If the stop criteria are satisfied, the procedure comes to a stop, or else goes to the ***Step 2***.

In this paper, the use of global model in NBPSO is considered, and the parameters in (5.10) are set as the same as Ref. [92]. Usually v_{max} is set to be 6, $c_1=c_2=2$ and the weight w is decreasing linearly from 0.6 to 0.2. The number of particle (N_P) is 20, and the length of bit in each particle (P) is 32. The number of iteration (T) is considered to be 30, which is the stopping criteria.

5.3 Experimental setup and results

5.3.1 Experimental setup

Figure 5.3 shows the experimental setup of the NBPSO based on DSI method in the IM-DD optical OFDM system.

In the experiment, three types of signal are used such as the original OFDM signal, the DSI signal, and the NBPSO based on the DSI signal. The parameters of experiment are shown in the Table 1.

The pseudo-random binary sequence (prbs) is converted into parallel data by S/P converter, and then the NBPSO based on DSI method is processed for PAPR reduction. The algorithm of NBPSO include a loop: add a dummy sequence into the end of the each parallel data, and then they are mapped into 16QAM modulation. After that add GI and Hermitain constrains. Then the data symbol is passed through the IFFT, and PAPR is calculated. After the NBPSO method implemented, the signal with min PAPR is obtained. A complex-valued time domain waveform is produced, meanwhile, the CP is added to mitigate the ISI. In addition, a training sequence (TS) can be used for channel estimation and symbol synchronization. The electrical base-band OFDM signals are generated by offline Matlab, and they are uploaded into a commercial arbitrary waveform generator (AWG). The sample rate of the AWG is 5 GSamples/s. The peak-to-peak voltage of the signals is 1V. A continuous wave (CW) light wave is generated from an external cavity laser (ECL) at a wavelength of 1556.26 nm and line-

width of 100 kHz with output power of 14.5 dBm. After MZM, the output power of optical OFDM signals is 2 dBm. The optical OFDM signals are amplified by the first EDFA (EDFA1) before transmitted over 100 km SMF. After transmission over 100 km SSMF, the second EDFA (EDFA-2) and a variable optical attenuator (VOA) are adopted for controlling the received power. The optical OFDM signals are converted into electrical wave signals via a PIN photodiode, then passed through the LPF and recorded by real-time digital storage oscilloscope (TDS-6804B).
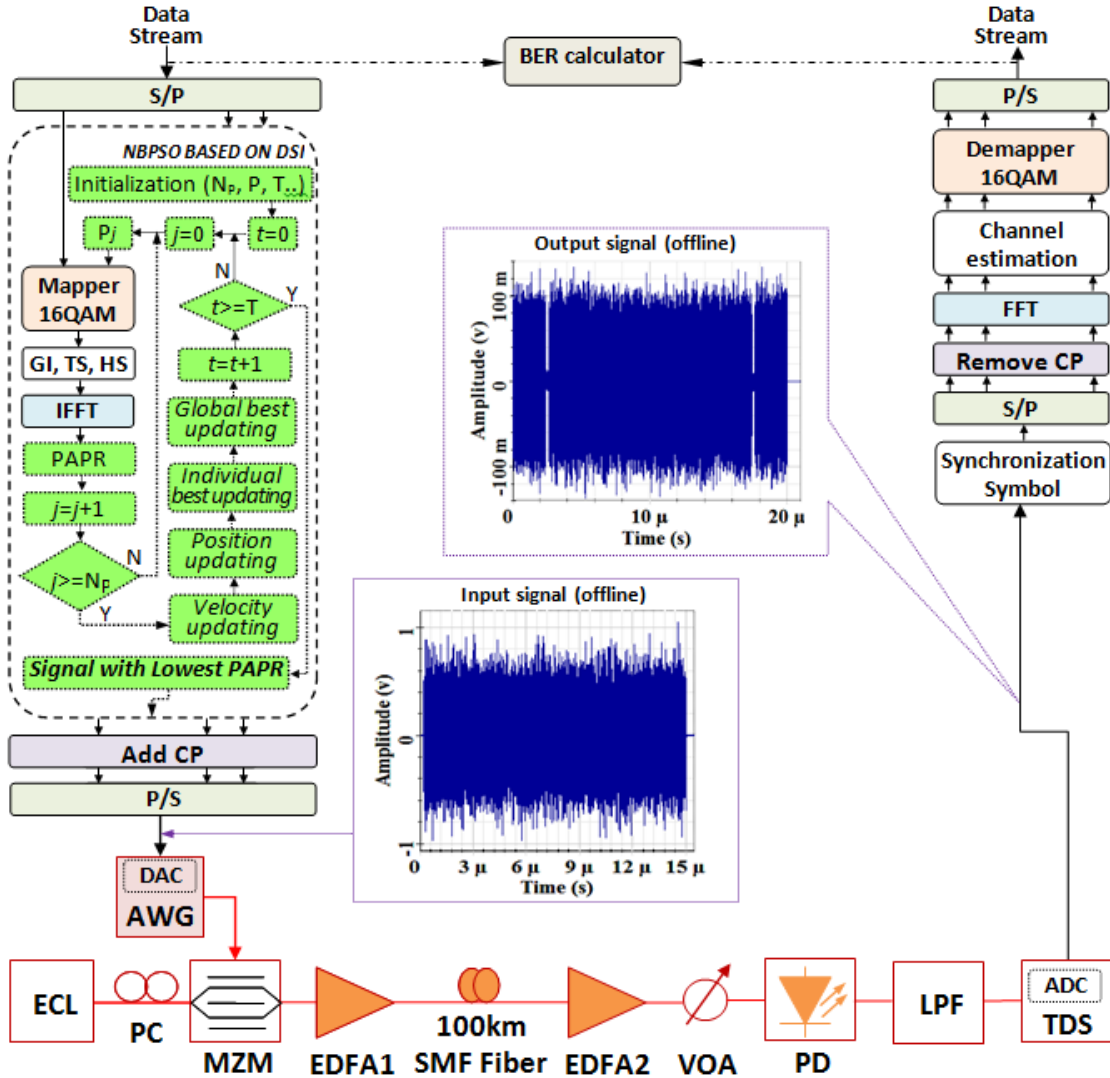
Figure 5.3: The experimental setup for the IM-DD OFDM system with the NBPSO based on DSI method. VOA: variable optical attenuator, ECL: external cavity laser, PC: polarization controller, MZM: Mach–Zehnder modulator, EDFA: Erbium doped fiber amplifier, PD: photodiode, TDS: Real time/digital storage oscilloscope and LPF: low pass filter.

At the receiver, the signals are processing as the same as the original OOFDM system. The waveform recorded by TDS is processed by offline Matlab. The channel estimation and the symbol synchronization are realized by using training sequence (TS).

The TS is similar to Park's method [78]. And the synchronization symbol is realized by Chen et al [79], and the channel estimation is calculated by linear interpolation [80]. Finally, BER performances of the received signals are calculated.

Table 5.1: The parameters of experiment

Items	Sub items	Value
OFDM	FFT	256
	Subcarriers for data	184
	Subcarriers for DSI	16
	CP	32
	PRBS length	94208
	Modulation	16QAM
	OFDM symbol	256
Training sequence	Training sequence	1
ECL	Power output (dBm)	14.5
	Wavelength (nm)	1556.26
	Line-width (kHz)	100
MZM	Half-wave voltage (V)	4
	Bias voltage (V)	2.4
	Power output (dBm)	2
Fiber	Fiber length (km)	100
	Attenuation (dB/km)	0.19
	Dispersion (ps/nm/km)	16.75
	Dispersion slope (ps/nm^2/km)	0.075
	Effective area (um^2)	80
	n_2 (m^2/w)	2.6e-20
	SNR (dB)	15
AWG	Sample rate (GSa/s)	5
	Vpp (v)	1
PD	Wavelength range (nm)	1280
	Bandwidth (GHz)	10
LPF	3-dB bandwidth (GHz)	2
EDFA	Wave length range (nm)	1530-1560
	Noise Figure	Max. 5dB
TDS	Sample rate (GSa/s)	10

5.3.2 Experiment results and discussions

The net bit rate of data signal is 92 x 4 x 256/((1000 + 257 x 288) x 0.2) $\approx$ 6.23 (Gb/s), and the net bit rate of dummy sequence signal is 8 x 4 x 256/((1000 + 257 x 288) x 0.2) $\approx$ 0.546 (Gb/s). In this way, the transmission efficiency is calculated as: Subcarriers for data /(Subcarriers for DSI + Subcarriers for data) (%) = 92/(8 + 92)(%) = 92%.

Figure 5.4 shows the CCDF versus PAPR of OFDM signal, NBPSO based on DSI signal, and DSI signal with the threshold of 12 dB. At the CCDF of 10^{-4}, the PAPR of the OFDM signal with the NBPSO based on DSI method is reduced by 2.8, and 1.4dB compared with that of the original OFDM and the DSI with threshold of 12 dB, respectively.
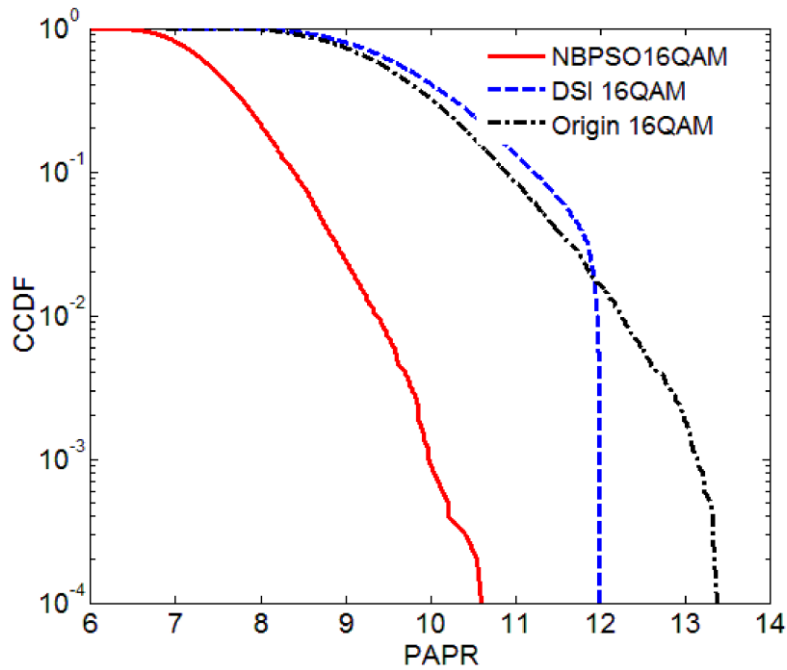
Figure 5.4: Complementary cumulative distribution function (CCDF) versus peak to average power ratio (PAPR) of OFDM signals.

The BER performance of original OFDM signal, DSI signal and NBPSO based on DSI signal with 2 dBm of fiber launch power after transmission over 100 km SMF is shown in Figure 5.5. At the BER of FEC 3.8×10^{-3}, the received optical power is about -4.8 dBm for that with NBPSO based on DSI method, -3.7 dBm for that with the DSI method, and -2.9 dBm for original OFDM signal. The received sensitivity of OFDM signal with the NBPSO based on DSI method can be improved by 1.1 dB, and 1.9 dB when compared with that of the DSI method, and original OFDM, respectively.

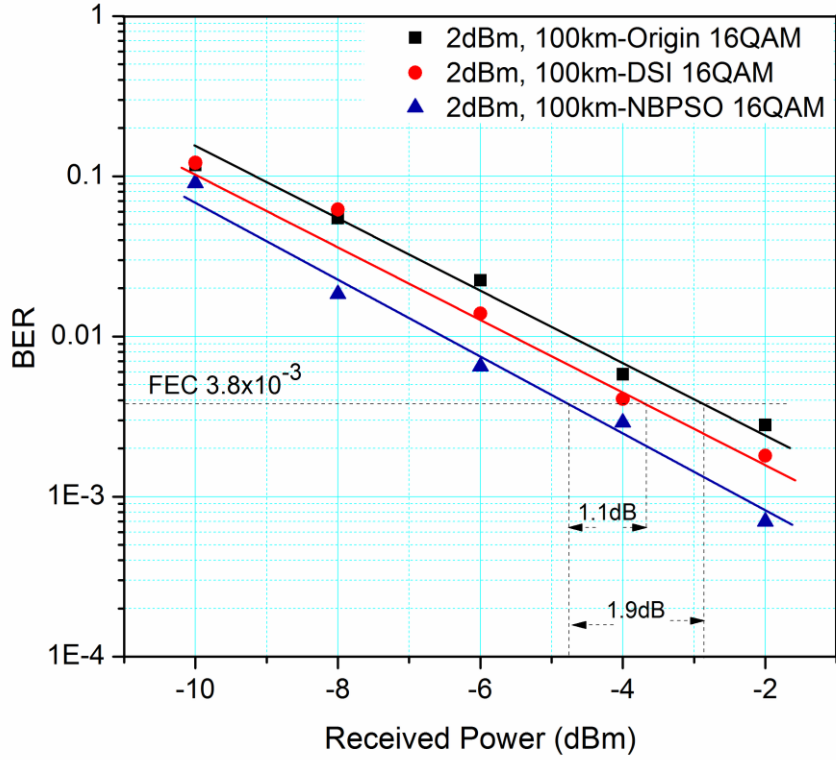Figure 5.5: BER curves of OFDM signals at 2 dBm launch power
after transmission over 100km SMF.
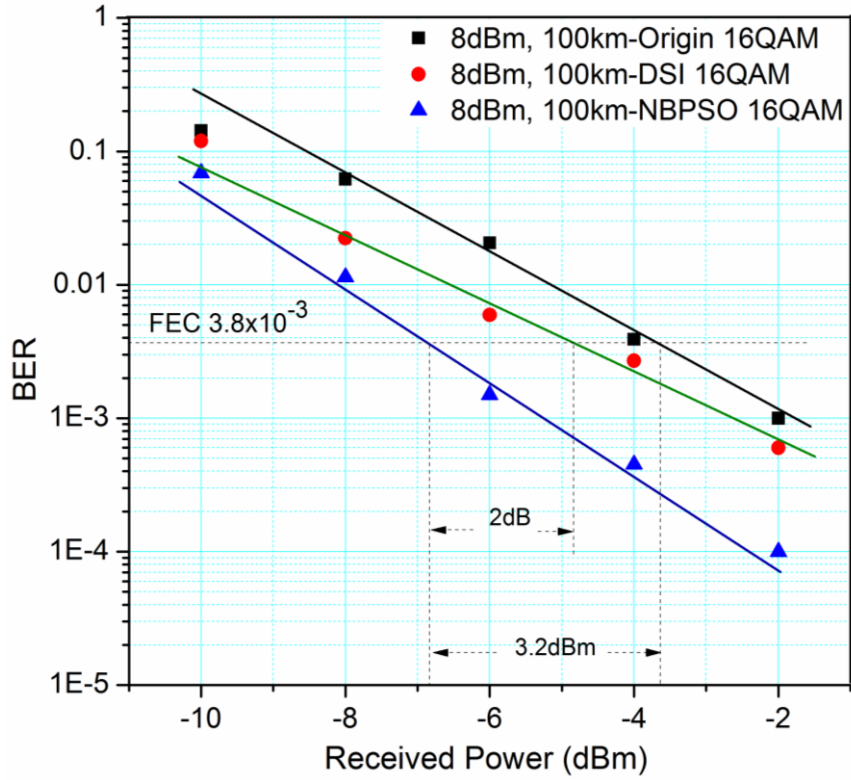
Figure 5.6: BER curves of OFDM signals at 8 dBm launch power
after transmission over 100 km SMF.

The BER performance of OFDM signals with received power is shown in Fig. 6. At the BER of FEC 3.8×10^{-3}, the received optical power of NBPSO based on DSI signal, the DSI signal and original signal is about -6.8, -4.8 and -3.6 dBm, respectively. The received sensitivity with NBPSO based on DSI method can be improved by 2 dB, and 3.2 dB when compared with the case of DSI method, and original OFDM, respectively.

Figure 5.7 shows BER via fiber launch power of optical OFDM signals at received optical power of -2 dBm after transmission over 100 km SMF. At the same launch power, BER performance of the proposed technique is the best, BER performance of original is the worst. As the launch power increasing from 2 dBm to 8 dBm, BER of all optical OFDM signal are decreasing. Meanwhile, the BER of the proposed technique is faster decreasing than that of the other techniques. The BER of 8dBm to fiber is lower than that of 2dBm to fiber, it means that there is no effect of the nonlinear. The BER of all optical OFDM signals are the min value as the launch power is about 8dBm. Moreover, with the launch power increasing from 8 dBm to 11 dBm, the BER of all optical OFDM signal is increasing, but the BER performance of the proposed technique is better than that of the other techniques. When the power to fiber is more than 8dBm, there is nonlinear effect. The experimental results indicate that the proposed technique can resist nonlinear. And it is better than other techniques.

Figure 5.7: BER via launch power of OFDM signals after transmission over 100 km SMF.

5.4 Conclusion
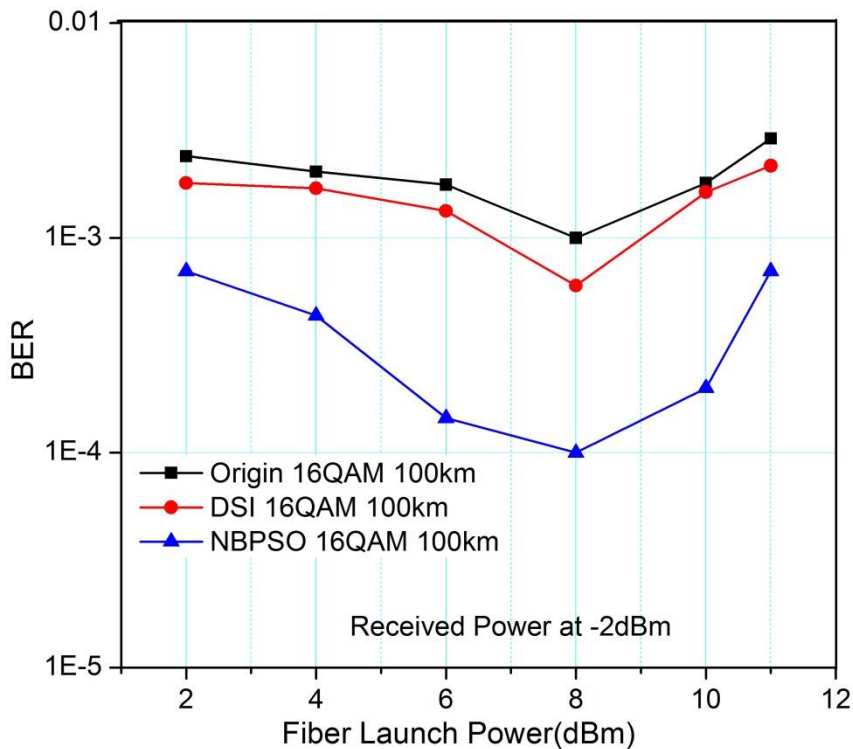
In this paper, we proposed and experimentally demonstrated a novel NBPSO based on DSI method in the IM/DD OOFDM system. The novel proposed technique was used to reduce the fiber nonlinear effect through reducing the PAPR of the OFDM signal. The experimental results showed that at the same launch power, the received sensitivity of the optical OFDM signal with the proposed technique (just with a small of particles and iterations) is better than that of the signal with DSI method and with the original OFDM. At the CCDF of 10^{-4}, the PAPR of OFDM signal with the proposed technique was reduced by 1.4 and 2.8 dB with the DSI method and with the original OFDM, respectively. At a BER of FEC limitation 3.8×10^{-3}, the received power with proposed technique was more sensitive than that of the original OFDM. Thus, by using the proposed technique, it can reduce the fiber nonlinear effect efficiently.

Compared to PAPR reduction scheme based on new spreading code in chapter 3, and the hybrid method in chapter 4, the NBPSO based DSI method can slightly reduce the PAPR and can get BER performance less than other two methods above. At the CCDF of 10^{-4}, the PAPR of OFDM signal with the NBPSO is reduced by 2.8dB, while with the hybrid method is reduced by 5.7 dB and with the new spreading code method is reduced by 4.6 dB when compared to the original OFDM. The experimental results also indicated that, at the smaller BER limit FEC, the receiver sensitivity of the optical OFDM signal of the NBPSO is also smaller than the hybrid method and the new spreading code when compared to origin signal. But at the receiver side, the hardware of the NBPSO method is the same as the original system. Meanwhile the signals at receiver side of hybrid method and the new spreading code is multiplied with a matrix C*[N,N], and matrix of [2N+1,N], respectively.

Chapter 6: **CONCLUSION AND FUTURE WORK**

6.1 Summary of the work

In this thesis, we explained theoretical and realized experiment on Intensity Modulator/Direct Detection (IM/DD) optical OFDM systems. The most important drawbacks of IM/DD optical OFDM system have been considered and focus was placed on techniques such as the PAPR of the OFDM signal and the frequency offset and phase noise. We first proposed and experimentally demonstrated an IM/DD optical OFDM with new spreading code for PAPR reduction. We then developed a new hybrid based on carrier interferometry combined with companding transform for PAPR reduction. Finally, we designed an IM/DD optical OFDM system which reduces the PAPR based on new particle swarm on dummy sequence insertion without side information. The main contributions are:

1. A novel technique for PAPR reduction in IM/DD optical OFDM system based on new spreading code is proposed. The new spreading code with low cross-correlation and high auto-correlation while capable of supporting $2N+1$ users or data symbols is investigated. The proposed technique is experimentally demonstrated over 70 km SMF transmission with number of subcarrier is 256 and 512. The results shown that, the proposed technique can reduce the PAPR and improve the received sensitivity compared with original system. The result also prove that new spreading code has better orthogonality property proportional to the high number of subcarrier. With the same subcarrier, at the BER of 1×10^{-3} for 1.726 Gb/s BPSK proposed signal and 1.718 Gb/s 4QAM original signal, the receiver sensitivity of proposed signal can improve by 2.1 dB, with fiber launch power of 2.75 dBm. The PAPR can reduce by about 4.6 dB, compared with the original OFDM signal at a CCDF of 10^{-4}.

2. a new hybrid technique is proposed for PAPR reduction in IM/DD optical OFDM system. This hybrid based on CI codes combined with companding transform. The brief structure of CI codes and companding transform are presented, and an end to end signal processing is mathematically investigated. The effect of our proposed hybrid in the BER performance of the system has been experimentally demonstrated over 100 km SMF with different launch

powers. At a CCDF of 10^{-4}, the PAPR of OFDM signal with the hybrid technique is reduced by 5.7 dB, while with the CI codes and the companding technique are reduced by 3.1 and by 2.8 dB, respectively comparing with the original OFDM. The experimental results show that, at the same fiber launch power, the receiver sensitivity of optical OFDM signal with the hybrid technique is better than signal with CI codes, with companding technique and with the original OFDM. At the BER of 10^{-4} for 1.718 Gb/s 4QAM signals, the received power of optical OFDM signal with hybrid technique is more sensitive than the original OFDM by 3.7, 4.2, and 5 dB in case of 3, 6, 9 dBm fiber launch power, respectively. It can be clearly seen that the proposed system can improve the received sensitivity when the optical launch power is increasing

3. A novel binary particle swarm optimization (NBPSO) method based on dummy sequence insertion (DSI) is proposed and experimentally demonstrated for PAPR reduction in the IM/DD OOFDM system. The specified dummy sequence is inserted only for PAPR reduction and without any side information. The key to enhance its performance is creating more qualified dummy sequence. The novel binary particle swarm optimization method can find more qualified dummy sequence. In this way, it can be used to mitigate the PAPR problem in OFDM system effectively. The experiment results show that, at the BER of FEC 3.8×10^{-3} for 6.23 Gb/s 16QAM signals after transmission over 100km SMF, the improvement of the receive sensitivity by the proposed scheme is 1.9 and 3.2 dB in case of 2 and 8 dBm launch power, respectively. At the CCDF of 10^{-4}, the PAPR reduced by more 2.8 dB when compared to conventional system.

6.2 Future work

The main proposed techniques have been efficient for the Intensity Modulator/Direct Detection optical OFDM system. We intend to improve the system performance by taking account the following points

1. High sampling rate

2. Recovering algorithm at the receiver side

3. Joint our techniques to the well know PAPR reduction techniques

We planned to apply our proposed techniques in more advanced and complex optical OFDM systems such as:

1.   Real time optical OFDM system

2.   Coherent optical OFDM system

3.   OFDM-Radio Over fiber system

4.   Fast OFDM system

ACKNOWLEDGEMENTS

First of all, I would like to express my deep and sincere gratitude and appreciation for my supervisor, Prof LIN CHEN, for his advice, patience, continuous support and guidance during my doctoral program at Hunan University. Prof CHEN always paid attention of his students work. He was always accessible and aimed exceptional work. His wide knowledge and logic way of thinking have been a great value for me.

I am also very grateful to my associate advisor Prof He Jing for his assistant, support, useful comments for the successful of this thesis.

Many thanks go to the colleagues in our Optical OFDM group, Chen Ming, Tang Jing, Mangone Fall, Rui Deng for constructive suggestions, ideas, discussions we shared during our group meeting over the last three years.

I wish to express my warm and sincere thanks to all my friends at Hunan University and around china for their help and support during my study program.

Last, and most importantly, I am very grateful to my family, for their encouragements, support and sacrifices throughout all my life. I also wish to express my special thanks to my wife, who dedicatedly takes care of our children while I am away studying.

REFERENCES

[1] Lowery A J, Liang D, and Armstrong J. Orthogonal frequency division multiplexing for adaptive dispersion compensation in long haul WDM systems. In: Proc of OFC/NFOEC 2006, Anaheim, CA, USA 2006, 3.

[2] Djordjevic I B, and Vasic B. Orthogonal frequency division multiplexing for high-speed optical transmission. Opt. Express, 2006, 14(9): 3767-3775.

[3] Shieh W, and Djordjevic I B. OFDM for optical communications. Academic Press, 2009.

[4] Shieh W, Yi X, and Tang Y. Transmission experiment of multi-gigabit coherent optical OFDM systems over 1000km SSMF fiber. Electron. Lett, 2007, 43(3): 183-184.

[5] Goff D R, and Hansen K S. Fiber optic reference guide: a practical guide to communications technology. Focal Press, 2002

[6] Bulow H, Buchali F, Klekamp A. Electronic dispersion compensation. Journal of Lightwave Technology, 2008, 26(1-4): 158-167.

[7] Ali A, Paul H, Leibrich J, et al. Optical biasing in direct detection optical-OFDM for improving receiver sensitivity. In: Proc of OFC/NFOEC, 2010, 1-3.

[8] Shieh W, Bao H, and Tang Y. Coherent optical OFDM: theory and design. Opt Express, 2008, 16(2): 841-59.

[9] Schmidt B, Lowery A J, Armstrong J. Experimental demonstrations of 20 Gbit/s direct-detection optical OFDM and 12 Gbit/s with a colorless transmitter. Optical Fiber Communication Conference, 2007.

[10] Djordjevic I B, Vasic B. Orthogonal frequency-division multiplexing for high-speed optical transmission. Opt. Express, 2006, 14(3): 767-3775.

[11] Gao Y, Yu J, Xiao J, et al. Direct-Detection Optical OFDM Transmission System With Pre-Emphasis Technique. J. Lightw. Technol, 2011, 29(14): 2138–2145.

[12] Jansen S L, Morita I, Schenk T, et al. Coherent optical 25.8-Gb/s OFDM transmission over 4160-km SSMF. J. Lightw. Technol, 2008, 26(1): 6-15.

[13] Cvijetic N. OFDM for next-generation optical access networks. J. Lightwave Technol., 2012, 30(4): 384-398.

[14] Shen G, Zukerman M. Spectrum-Efficient and Agile CO-OFDM Optical Transport Networks: Architecture, Design, and Operation. IEEE Communications Magazine, 2012, 50(5): 82-89.

[15] Lowery A J, Du L, Armstrong J. Orthogonal frequency division multiplexing for adaptive dispersion compensation in long haul WDM systems, In: OFC 2006 Anaheim, CA, 1-3.

[16] Armstrong J. OFDM: From copper and wireless to optical, In: OFC/NFOEC, San Diego, CA, 2008, 1-27.

[17] Chang C W. Orthogonal frequency multiplex data transmission system. 1996.

[18] Salz J, Weinstein S B. Fourier transform communication system. In: Proc of ACM Symp. Problems Optim. Data Commun. Syst, Pine Mountain, GA,USA, 1969.

[19] Peled A, Ruiz A. Frequency domain data transmission using reduced computational complexity algorithms, In: IEEE International Conference on ICASSP'80, 1980, 964-967.

[20] Telatar I E. Capacity of Multi-Antenna Gaussian Channels. Tech European Trans. Telecommun, 1999, 10(6): 585-595.

[21] Foschini G J, and Gans M J. On limits of wireless communications in a fading environment when using multiple antennas. Wireless Pers. Commun, 1998, 6(3): 11-335.

[22] CiminiJr L. Analysis and simulation of a digital mobile channel using orthogonal frequency division multiplexing. Communications, IEEE Transactions on, 1985, 33(7): 665-675.

[23] Lassalle R R, Alard M. Principles of modulation and channel coding for digital broadcasting for mobile receivers. EBU Tech. Rev, 1987, 224(1): 68-190.

[24] Chow J S, Tu J C, Cioffi J M. A discrete multitone transceiver system for HDSL applications. IEEE J. Sel. Areas Commun, 1991, 9(8): 95-908.

[25] Koffman I, Roman a. Broadband wireless access solutions based on OFDM access in IEEE 802.16. IEEE Commun. Mag, 2002, 40: 96-103.

[26] Reimers I. Digital video broadcasting. IEEE Commun. Mag, 1998, 36: 104–110.

[27] Gurprakash S, Arokiaswami A. OFDM Modulation Study for a Radio-over-Fiber Systemfor Wireless LAN (IEEE 802.11a), In: IcIcs-F'CMZW3 2003, 15-18.

[28] Fan S, Yu J, Chang G. Optical OFDM scheme using uniform power transmission to mitigate peak-to-average power effect over 1040 km single mode fiber. J. Opt. Commun. Netw, 2010, 2: 711–715.

[29] Fyath R S, Al-mfrji A. Performance Evaluation of Multimode Fiber-Based Optical OFDM Communication System, In: The 1st Regional Conference of Eng.Sci. NUCEJ Spatial, 2008, 70-83.

[30] Geng L, Penty R, V, White I, H, et al. FEC-free 50 m 1.5 Gb/s plastic optical fibre link using CAP modulation for home networks, In: ECOC, 2012, Paper Th.1.B.4.

[31] Jianming T, Roger G, Xianqing J, et al. Real-time optical OFDM transceivers for PON applications. Optical Fiber Communication Conference, 2011, OTuK3.

[32] Nee R V, and Prasad R. OFDM for wireless multimedia communications. Artech House Publishers, 1999.

[33] Weinstein S B, and Ebert P M. Data transmission by frequency division multiplexing using the discrete Fourier transform. IEEE Trans. Commun. Technol, 1971, 19(5): 628-634.

[34] Bailey D H, and Swarztrauber P N. The fractional Fourier transform and applications. Society for Industrial and Applied Mathematics Review, 1991, 33(3): 389-404.

[35] Hara S, Prasad R. Multicarrier Techniques for 4G Mobile Communications, 2003

[36] Armstrong J. OFDM for optical communications. J. Lightw. Technol, 2009, 27(3): 189-204.

[37] Li X, Cimini L J. Effect of clipping and filtering on the performance of OFDM. IEEE Commun. Letter, 1998, 2(5): 131-133.

[38] Muller S H, Huber J B. A comparison of peak power reduction schemes for OFDM, In: IEEE Global Communications Conference (GLOBECOM), Phoenix, AZ, 1997, 1-5.

[39] Bäuml R W, Fisher R F H, Huber J B. Reducing the peak-to-average power ratio of multicarrier modulation by selected mapping. IEE Electronic Letters, 1996, 32(22): 2056-2057.

[40] Muller S H, Huber J B. OFDM with reduced peak-to average power ratio by optimum combination of partial transmit sequences. IEE Electronic Letters, 1997, 33(5): 368-369.

[41] Cimini L J, Sollenberger N R. Peak-to-average power ratio reduction of an OFDM signal using partial transmit sequences. IEEE Communications Letters, 2000, 4(3): 86-88.

[42] Jayalath A D S, and Tellambura C. An adaptive PTS approach for the reduction of peak-to-average power ratio of an OFDM signal. IEEElectronic Letters, 2000, 36(14): 1226-1228.

[43] Wiegandt D A, Nassar C R, Wu Z Q. Overcoming peak-to-average power ratio issues in OFDM via carrier-interferometry codes. In: Proc of Ieee 54th Vehicular Technology Conference, Vtc Fall 2001, Vols 1-4, Proceedings, 2001, 660-663.

[44] Anwar K, Saito M, Hara T, et al. New Spreading Codes for MC-CDMA and OFDM Systems. In: Proc of Proceedings of the 11th IEEE Symposium on Computers and Communications (ISCC'06), 2006.

[45] Heung-Gyoon R, Jae-Eun L, and Jin-Soo P. Dummy sequence insertion (DSI) for PAPR reduction in the OFDM communication system. IEEE Trans. on Consum. Electron, 2004, 50(1): 89-94.

[46] Kumar M U R, Daula S M S. Analysis of PAPR of DHT-Precoded OFDM System for M-QAM. International Journal of Engineering Research and Applications, 2012, 2(2): 604-608.

[47] WANG Z-p, CHEN F-n, WU M-w, et al. Experimental evaluation of the BER performance in optical OFDM system based on discrete Hartley transform precoding. OPTOELECTRONICS LETTERS, 2012, 10(3): 0224-0227.

[48] Davis J A, and Jedwab J. Peak-to-mean power control in OFDM, Golay complementary sequences, and Reed-Muller codes, In: IEEE Trans. Inf. Theory, 1999, 2397-2417.

[49] Jones E, Wilkinson T A, Barton S K. Block coding scheme for reduction of peak to mean envelope power ratio of multicarrier transmission scheme. IEE Electronic Letters, 2004, 30(22): 2098–2099.

[50] Jiang T, Zhu G. Complement block coding scheme for reducing peak-to-average power ratio of OFDM systems. J. Electronics, 2004, 21(5): 413-420.

[51] Jones D. Peak power reduction in OFDM and DMT via active channel modification, In: 33rd Asilomar Conference on Signals, Systems, and Computers, 1999, 1076–1079.

[52] Tellado J, and Cioffi J M. Multicarrier Modulation with Low PAR, Application to DSL and Wireless, Boston. 2000.

[53] Kim D, and Stuber G L. Clipping noise mitigation for OFDM by decision-aided reconstruction. IEEE. Commun. Lett, 1999, 3(1): 4-6.

[54] Ali A, Al-Rabah A, Masood M, et al. Receiver-Based Recovery of Clipped OFDM Signals for PAPR Reduction: A Bayesian Approach. IEEE access, 2014, 2: 1312-1324.

[55] Xianbin W, Tjhung T T, Ng C S. Reply to the comments on "Reduction of peak-to-average power ratio of OFDM system using a companding technique". IEEE Transactions on Broadcasting, 1999, 45(4): 420-422.

[56] Ren G L, Zhang H N, Chang Y L, et al. A self companding transform to.reduce peak-to-average power ratio in OFDM based WLANs. In: Proc of 2006 International Conference on Communications, Circuits and Systems Proceedings, Vols 1-4, GuiLin, 2006, 1142-1146.

[57] Huang X, Lu J, Zheng J, et al. Companding Transform for Reduction in Peak-to-Average Power Ratio of OFDM Signals. IEEE Transactions on Wireless Communications, 2004, 3(6): 2030-2039.

[58] Wang X B, Tjhung T T, and Ng C S. Reduction of peak-to-average power ratio of OFDM system using a companding technique. IEEETrans.Broadcasting, 1999, 45(3): 303-307.

[59] Van N R, and De W A. Reducing the peak-to-average power ratio of OFDM, In: in Proc. IEEE Vehicular Technology Conference, 1998, 2072-2076.

[60] Huang Y, Zeng Z. A Simplified Peak Cancellation Method for OFDM Signals, In: Computer Science and Electronics Engineering (ICCSEE), 2012, 336-339.

[61] Armstrong J. Analysis of new and existing methods of reducing in-ter carrier interference due to carrier frequency offset in OFDM IEEE Trans. Commun. Technol, 1999, 47: 365–369.

[62] Li Y, Cimini L J, Jr. Bounds on the interchannel interference ofOFDM in time-varying impairments. IEEE Trans. Commun., 2001, 49: 401-404.

[63] Pollet T, Van Bladel M, Moeneclaey M. BER sensitivity of OFDM systems to carrier frequency offset and Wiener phase noise. IEEE Trans. Commun., 1995, 43: 191-193.

[64] Garcia A A. Understanding the effects of phase noise in orthog-onal frequency division multiplexing (OFDM). IEEE Trans. Broad-casting, 2001, 47: 153-159.

[65] Omomukuyo O. Orthogonal Frequency Division Multiplexing for Optical Access Networks. University College London, 2013.

[66] Mynbaev D K, Scheiner L L. Fiber Optic Communications Technology. Prentice Hall, New Jersey, 2001

[67] Zhao B, Guo C X, and Cao Y J. A multi-agent-based particle swarm optimization approach for optimal reactive power dispatch. IEEE Transactions on Power Systems, 2005, 20(2): 1070-1078.

[68] Hsu D, Wei C, Chen H, et al. Cost-effective 33-Gbps intensity modulation direct detection multi-band OFDM LR-PON system employing a 10-GHz-based transceiver. Opt. Express, 2011, 19(18): 17546-17556.

[69] Schmidt B, Lowery A J, Armstrong J. Experimental Demonstrations of Electronic Dispersion Compensation for Long-Haul Transmission using Direct-Detection Optical OFDM. J. Lightwave Technology, 2008, 26: 196-203.

[70] Lowery A J, Armstrong J. Orthogonal-frequency-division multiplexing for dispersion compensation of long-haul optical systems. Opt. Expr, 2006, 14: 2079-2084.

[71] Yang Q, Tang Y, Ma Y, et al. Experimental demonstration and numerical simulation of 107-Gb/s high spectral efficiency coherent optical OFDM. J. Lightw. Technol, 2009, 27(3): 168-176.

[72] Masuda H Y E, Sano A, Yoshimatsu T, Kobayashi T, Yoshida E, Miyamoto Y, Matsuoka S, TakatoriY, MizoguchiM, Okada K,Hagimoto K, Yamada T, and Kamei S. 13.5-Th/s (135xIII-Gb/s/ch) no-guard-interval coherent OFDM transmission over 6248krn using SNR maximized second-order DRA in the extended L-band, In: Optical Fiber Communication INational Fiber Optic Engineers Conference (OFCINFOEQ), 2009, PDPB5.

[73] Jansen S L, Morita I, Schenk T, et al. Coherent optical 25.8-Gb/s OFDM transmission over 4160-km SSMF. J. Lightw. Technol, 2008, 26(1): 6-15.

[74] Biao Fu, Rongqing H. Fiber chromatic dispersion and polarization-mode dispersion monitoring using coherent detection. IEEE Photon. Technol. Lett, 2005, 17: 1561-1563.

[75] Leibrich J, Ali A, Paul H, et al. Impact of modulator bias on the OSNR requirement of direct-detection optical OFDM. IEEE Photon. Technol. Lett, 2009, 15: 1033–1035.

[76] Hou J, Ge J, Zhai D, et al. Peak-to-average power ratio reduction of OFDM signals with nonlinear companding scheme. IEEE Trans. Broadcas, 2010, 56(2): 258–262.

[77] Park M, Heeyong J, Cho N, et al. PAPR reduction in OFOM transmission using Hadamard transform, In: IEEE International Conference on Communications, 2000, 430-433.

[78] Park B, Cheon H, Kang C, et al. A novel timing estimation method for OFDM systems. Ieee Communications Letters, 2003, 7(5): 239-241.

[79] Chen M, He J, Cao Z, et al. Symbol synchronization and sampling frequency synchronization techniques in real-time DDO-OFDM systems. Optics Communications, 2014, 326: 80-87.

[80] Chen M, He J, Chen L. Real-Time Optical OFDM Long-Reach PON System Over 100 km SSMF Using a Directly Modulated DFB Laser. Journal of Optical Communications and Networking, 2014, 6(1): 18-25.

[81] Wang J, Guo Y, Zhou X. PTS-Clipping Method to Reduce the PAPR in ROF-OFDM System. IEEE Transactions. Consumer. Electronics, 2009, 55(2): 356-359.

[82] Xiao J N, Yu J, Li X, et al. Hadamard transform combined with companding transform technique for PAPR reduction in an optical direct-detection OFDM system. Optical Communications and Networking, 2012, 4(10): 709-714.

[83] Mangone F, Tang J, Chen M, et al. Iterative clipping and filtering based on discrete cosine transform/inverse discrete cosine transform for intensity modulator direct detection optical orthogonal frequency division multiplexing system. Optical Engineering, 2013, 52(6): 065001-6.

[84] Mangone F, He J, Tang J, et al. A PAPR reduction technique using Hadamard transform combined with clipping and filtering based on DCT/IDCT for IM/DD optical OFDM systems. Optical fiber technology journal, 2014, 20(4): 384-390.

[85] Maivan L, He J, Chen M, et al. New hybrid peak-to-average power ratio reduction technique based on carrier interferometry codes and companding technique for optical direct-detection orthogonal frequency division multiplexing system. Optical Engineering, 2014, 53(8): 086104-7.

[86] Wu Z Q, Wu Z J, Wiegandt D A, et al. High-performance 64-QAM OFDM via carrier interferometry spreading codes. In: Proc of 2003 Ieee 58th Vehicular Technology Conference, Vols1-5, Proceedings, 2003, 557-561.

[87] Ali A, Leibrich J, Rosenkranz a W. Carrier-Interferometry-OFDM for Nonlinear Tolerance Improvement in Optical Systems with Direct Detection. Photonic Networks, 14. 2013 ITG Symposium. Proceedings, 20131-5.

[88] Chen H X, Yu J J, Xiao J N, et al. Nonlinear effect mitigation based on PAPR reduction using electronic pre-distortion technique in direct-detection optical OFDM system. Optical Fiber Technology, 2013, 19(5): 387-391.

[89] Li F, Yu J, Cao Z, et al. Reducing the peak-to-average power ratio with companding transform coding in 60 GHz OFDM-ROF systems. Optical Communications and Networking, 2012, 4(3): 202-209.

[90] Fort A, Weijers J W, Derudder U, et al. A performance and complexity comparison of auto-correlation and cross-correlation for OFDM burst synchronization. In: Proc of Ieee International Conference on Acoustics, Speech, and Signal Processing, Vol Ii, Proceedings, 2003, 341-344.

[91] Zou W, Yu J, Xiao J, et al. Direct-detection Optical Orthogonal Frequency Division Multiplexing System with New Training Sequence. Frequenz, 2012, 66(1-2): 27-32.

[92] Nezamabadi-pour H, Rostami-sharbabaki M, Maghfoori-Farsangi M. Binary Particle Swarm Optimization: Challenges and New Solutions. Journal of Computer Society of Iran (CSI) On Computer Science and Engineering (JCSE), 2008, 6(1): 12.

[93] Kim S W, Byeon H S, Kim J K, et al. An SLM-based Real-time PAPR Reduction Method Using Dummy Sequence Insertion in the OFDM Communication. In: Proc of Fifth Int. Conf. on Information, Comm. and Sig. Proc., pp.258-262, Dec., 2005, Bangkok, 2005, 258-262.

[94] Kennedy J, Eberhart R. Particle swarm optimization. In: Proc of Neural Networks, Proceedings, IEEE International Conference on 1995, 1942-1948.

[95] Kennedy J, Eberhart R C. A discrete binary version of the particle swarm algorithm, In: IEEE International Conference on Computational Cybernetics and Simulation, 1997, 4104-4108.

[96] Huang C M, Huang C J, and Wang, M L. A particle swarm optimization to identifying the ARMAX model for short-term load forecasting. IEEE Transactions on Power Systems, 20(2), , 2005, 20(2): 1126-1133.

[97] Zhao B, Guo C X, and Cao Y J. A Multi-agent-Based Particle Swarm Optimization Approach for Optimal Reactive Power Dispatch. IEEE Transactions on Power Systems, 2005, 20(3): 1663 – 1663.

[98] Lip H B, Tang Y Y, Meng J, et al. Neural networks learning using vbest model particle swarm optimization. In: Proc of Proceedings of the 3rd International Conference on Machine Learning and Cybernetics, Shanghai, China, 2004.

[99] Al-kazemi B, and Mohan C. Training feed forward neural networks using multi-phase particle swarm optimization. In: Proc of Proceedings of the 9th International conference on Neural Information(5), 2002.

[100] Merwe D, and Engelbrecht A. Data clustering using particle swarm optimization. http://cirg.cs.up.ac.za/publications/ CEC2003d.pdf. 2003.

[101] Gudise V G, and Venayagamoorthy G K. FPGA placement and routing using particle swarm optimization. In: Proc of Proceedings of the IEEE Computer Society Annual Symposium on VLSI Emerging trends in VLSI Systems Design (ISVLSI'04). 2004.

[102] Sadeque S, Ahmed I, Vaughan R. Impact of individual and joint optimizations in multi-user OFDM resource allocation by modified PSO, In: Electrical and Computer Engineering (CCECE), 2011 24th Canadian Conference on, 2011, 001233 - 001237.

[103] Lee S-H, Hung H-L. Particle Swarm Optimization on DSI Method for PAPR Reduction in OFDM Systems, In: 2010 International Conference on Broadband, Wireless Computing, Communication and Applications, 2010, 639-642.

[104] Javad T, Ali A P, and Vahid T V. An Agent Based Particle Swarm Optimization for PAPR Reduction of OFDM Systems, In: 20th Telecommunications forum TELFOR 2012, Serbia, Belgrade, 2012, 839-842.

APPENDIX A: PUBLICATIONS

1. **Maivan Lap**, He Jing, Chen Ming, Mangone Fall, and Chen Lin. "**New hybrid peak-to-average power ratio reduction technique based on carrier interferometry codes and companding technique for optical direct-detection orthogonal frequency division multiplexing system**". *Optical Engineering, 2014, 53(8): 086104-7.*

2. **Maivan Lap,** He Jing, Chen Ming, and Chen Lin. " A PAPR reduction scheme based on a new spreading code in optical direct detection OFDM system". *Photonic Network Communication*. **(SCI – Accepted, 9.2015).**

3. **Maivan Lap,** He Jing, Deng Rui, and Chen Lin. "New binary Particle Swarm Optimization on Dummy Sequence Insertion Method for PAPR reduction in IM-DD OOFDM system". *Processing on Journal of Microwave and Optical Technology Letters*. (**SCI**)

APPENDIX B: SCIENTIFIC RESEARCH PROJECT DURING DOCTORAL STUDY

This thesis work is supported by:

1 The National "863" High Tech Research and Development Program of China (2011AA010203).

2 The Hunan Provincial Natural Science Foundation of China (12JJ3070)

3 The Open Fund of State Key Laboratory of Information Photonics and Optical Communications (Beijing University of Posts and Telecommunications).

4 The National Natural Science Foundation of China (Grant Nos. 61307087, 61377079)